IEEE Access
Multidisciplinary | Rapid Review | Open Access Journal

Received December 25, 2019, accepted January 11, 2020, date of publication January 21, 2020, date of current version January 28, 2020.

Digital Object Identifier 10.1109/ACCESS.2020.2968396

Super Twisting Disturbance Observer-Based Fixed-Time Sliding Mode Backstepping Control for Air-Breathing Hypersonic Vehicle

YUNJIE WU[1,2,3], FEI MA[1,2,3], XIAOCEN LIU[1,2,3], YUEYANG HUA[4], XIAODONG LIU[5], AND GUOFEI LI[1,2,3]

[1]State Key Laboratory of Virtual Reality Technology and Systems, Beihang University, Beijing 100191, China
[2]School of Automation Science and Electrical Engineering, Beihang University, Beijing 100191, China
[3]Science and Technology on Aircraft Control Laboratory, Beijing 100191, China
[4]China Academy of Launch Vehicle Technology, Beijing 100076, China
[5]Beijing Aerospace Automatic Control Institute, Beijing 100854, China

Corresponding author: Fei Ma (mylovelylover26@163.com)

This work was supported by the National Natural Science Foundation of China under Grant 91216304 and Grant 61803357.

ABSTRACT This paper investigates the velocity and altitude tracking control problem for air-breathing hypersonic vehicle (AHV) under external disturbances and uncertainties. An improved smooth super-twisting based disturbance observer (SSTDOB) is proposed to estimate the unknown external disturbances. With the assistance of SSTDOB, an effective fixed-time sliding mode backstepping control (FSMBC) is designed to guarantee the tracking errors converge to a small neighbor of the origin. Meanwhile, a fixed-time tracking differentiator (FTD) is employed to estimate the virtual control inputs, which can eliminate the differential explosion problem. The overall stability of the closed-loop system is analyzed by utilizing Lyapunov stability theory. Simulation results demonstrate the effectiveness of the composite method.

INDEX TERMS Air-breathing hypersonic vehicle, backstepping control, disturbance observer, fixed-time sliding mode control, super twisting algorithm.

I. INTRODUCTION

Air-breathing hypersonic vehicle (AHV) usually flies at more than 5 Mach numbers in the near space region [1]. It has attracted tremendous attentions and numbers of researches due to the advantages of global response, strong penetration ability and great potential in military and civilian applications [2]. Compared with the conventional aircrafts, AHV can adopt scramjet engine as its main power and combine it with the body to realize the propulsion-airframe integration configuration [3]. Consequently, this integration would lead to heavy couplings among the elastic airframe, the propulsion system and the structural dynamics [4]. Moreover, the unmanageable nonlinear dynamics, the uncertainty of flight aerodynamic parameters and the severe external disturbances during the flight envelope would make the control of AHV more challenging [5]. Therefore, stability and robustness are still a focus issue of AHV.

The associate editor coordinating the review of this manuscript and approving it for publication was Shihong Ding.

In previous literatures, control approaches for the longitudinal dynamics of AHV can usually be divided into two parts: linear approaches and nonlinear approaches. The linearization technique plays an important role in classical flight control. With this technique, the linearized model of AHV about a specific trim condition can be obtained [6]. Sigthorsson *et al.* [7] proposed a robust linear output-feedback controller for AHV in the presence of model uncertainties and varying flight conditions. Gibson *et al.* [8] designed a control architecture containing gain-scheduling and integral control based nominal controller with adaptive strategy for AHV model under thrust and actuator uncertainties, which had shown the superior tracking performance of this controller. Besides, an improved linear-quadratic regulator (LQR) with fractional-order sliding mode control based tracking controller presented in [9] also exhibited excellent robustness for AHV under uncertainties.

However, the traditional linear control methods may show poor capability of providing desired control effect when the flight condition deviates far from the given trimming point.

This drawback can be overcome by some advanced nonlinear control methods, include fuzzy control [10]–[14], neural network control [15]–[21], sliding mode control [22]–[30] and backstepping control [18], [23], [24], [27], [38].

A T-S fuzzy model was adopted by Li *et al.* [10] to approximate the nonlinear dynamics of AHV. Then a robust adaptive fuzzy based tracking controller for HFV was developed to guarantee the stability of whole system with parameter uncertainty and unmodeled dynamics [11]. Furthermore, the mixed H_2/H_∞ robust fuzzy controller [13] and prescribed performance guaranteed cost fuzzy tracking control [14] for AHV were also investigated. In addition, Xu and Bu proposed a series of neural based controller for the longitudinal dynamics of hypersonic flight vehicle (HFV) [15]–[18]. With the help of these researches, many scholars extend this approximation technique to the controller design of HFV. For example, Xu *et al.* [20] combined the global neural control with dynamic surface control to achieve the stability of closed-loop HFV system and effectiveness of control scheme, where nonlinear functions of the HFV were approximated by the neural networks. Both fuzzy based controllers and neural based controllers can exhibit excellent approximation strength for unknown nonlinear functions.

Sliding mode control possesses excellent performance in convergence time and disturbance rejection. Thus, Xu *et al.* [23] combined the adaptive control strategies with sliding mode control, which can provide good tracking performance for the HFV under parametric uncertainty. In Zong *et al.* [24], a quasi-continuous high-order sliding mode controller based on full state feedback was designed for the longitudinal dynamics of flexible air-breathing hypersonic vehicles (FAHV), where the chattering problem was alleviated by introducing the quasi-continuous high-order sliding mode. To achieve the finite time stability of the control system, Sun *et al.* [27] proposed a finite time sliding mode control with disturbance observer for AHV. Besides, Yang *et al.* [28] developed a new nonsingular terminal sliding mode control (NTSMC) with backstepping strategy for FAHV, which can guarantee the finite time convergence and the steady-state precision. Moreover, since Polyakov [31] raised the fixed-time stability, this topic has been rigorously studied [32]–[34]. Zuo and Tie [35] addressed the fixed-time stable of first-order multi-agent systems. Basin *et al.* [36] considered the application of super-twisting based controller with fixed-time stability. Wang *et al.* [37] adopted the fixed-time backstepping scheme for AHV with external disturbances. For now, few literatures consider the fixed-time stability of AHV [38], [39], which would lead such problem still challenging.

Backstepping control (BC) is another effective nonlinear control design scheme. A series of aforesaid methods and the BC logic can be merged into an integral control framework with excellent ability to handle AHV's higher order nonlinear system. However, we cannot ignore the weak robustness and ''explosion of complexity'' of conventional BC. To enhance the robustness of controller, many disturbance observer (DOB) based techniques were investigated, such as fuzzy-based observer [12], [14], nonlinear disturbance observer [26], [40], [41], super twisting algorithm based observer [29], [30], extend state observer (ESO) [42], [43], etc. Li and Li [12] utilized a novel fuzzy-based approximator to estimate the total uncertainties of velocity subsystem and altitude system. Wu *et al.* [26] proposed a strictly-lower-convex-function constructing nonlinear disturbance observer (SDOB) based backstepping controller for HFV. Wang *et al.* [29] developed a conventional super-twisting algorithm to estimate the composite disturbances and uncertainties. An active disturbance rejection control (ADRC) based robust controller was employed for the AHV autopilot, where the ESO [42] was applied to estimate the parametric perturbations and atmospheric disturbances. In order to handle the differential explosion problem in BC, the dynamic surface control strategy was adopted by Xu *et al.* [20]. Bu *et al.* [21], [44] utilized a low-pass filter to transform the non-affine system to affine system so as to avoid the virtual control laws complexity involved in traditional BC strategy. Besides, some filter-based algorithms and differentiator-based algorithms [45], [46] can also get introduced to estimate the derivatives of virtual controls. Yu *et al.* [46] presented a novel finite-time command filter for the backstepping scheme, which can guarantee the finite time convergence property. Compared with conventional BC, these improved BC methods possess both higher tracking accuracy and better disturbance rejection ability.

Motivated by the above analysis, this study proposes a composite controller which consists of smooth super-twisting algorithm based disturbance observer (SSTDOB) and fixed-time sliding mode backstepping control (FSMBC) for AHV. Compared with the above literatures, the key innovative points of this paper are summarized as follows:

(1) The proposed SSTDOB is introduced for the equivalent disturbances of AHV, which has more general formulation for slow varying disturbance estimation and smoother outputs than that of conventional super twisting algorithms.

(2) The FSMBC has the merits of both fixed-time sliding mode control and dynamics surface control. The improved sliding surface can strength the states convergence speed and the bound of convergence time will be independent of AHV's initial conditions. The singularity problem caused by the derivative of virtual control is avoided by introducing a switching logic. Besides, all the system states are bounded and the ''explosion of complexity'' problem is avoided by utilizing a fixed-time tracking differentiator (FTD).

(3) The SSTDOB based FSMBC (SSTDOB-FSMBC) can guarantee the overall fixed-time stability of closed-loop system with faster response and higher tracking precision in the presence of external disturbances and uncertainties.

The remainder of this paper is organized as follows. Problem description section presents the longitudinal dynamics of AHV and the decomposed altitude subsystem and velocity subsystem. Then the SSTDOB is developed for the AHV system with the relevant stability analyzation at the same time.

The next section shows the main design process of SSTDOB-FSMBC, and the stability of composite method is also analyzed in detail. Besides, we implement two groups of simulation comparisons on an AHV. Eventually, the conclusion and future works are provided.

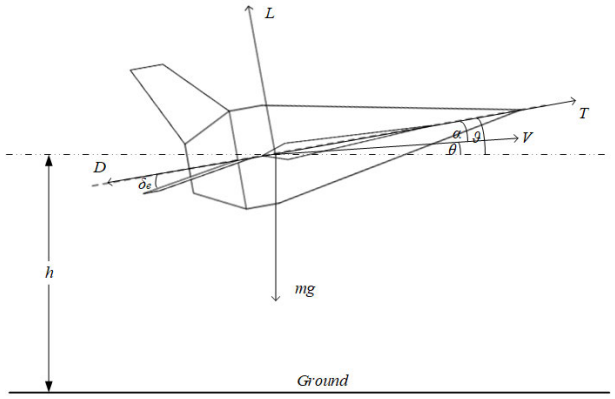

FIGURE 1. Schematic diagram for the longitudinal model of AHV.

II. PROBLEM DESCRIPTION

A. LONGITUDINAL DYNAMIC MODEL OF AHV

As is shown in Figure 1, the longitudinal dynamic model of a generic AHV [26], [29] consists of the following differential equations

$$\dot{h} = V \sin\theta \tag{1}$$

$$\dot{\theta} = \frac{L + T\sin\alpha}{mV} - \frac{\left(\mu - V^2(h+R_E)\right)\cos\theta}{V(h+R_E)^2} + d_2 \tag{2}$$

$$\dot{\vartheta} = \omega_z \tag{3}$$

$$\dot{\omega}_z = \frac{M_z}{J_z} + d_4 \tag{4}$$

$$\dot{V} = \frac{T\cos\alpha - D}{m} - \frac{\mu\sin\theta}{(h+R_E)^2} + d_5 \tag{5}$$

$$\alpha = \vartheta - \theta \tag{6}$$

where h, θ, ϑ, ω_z and V represent the altitude, path angle, pitch angle, pitch rate and velocity of the AHV respectively. μ, α, m, R_E and J_z denote the gravitation constant, angle of attack, mass of the AHV, radius of the earth and moment of inertia around AHV z axis, respectively. Besides, the terms d_i, $i = 2, 4, 5$, will indicate the external disturbances of each corresponding channel.

The thrust T, drag D, lift L and pitching moment M_z are expressed as follows

$$T = C_T qS \tag{7}$$

$$D = C_D qS \tag{8}$$

$$L = C_L qS \tag{9}$$

$$M_z = C_{m_z} qSl \tag{10}$$

where ρ, $q = \frac{1}{2}\rho V^2$, S and l represent the density of air, dynamics pressure, reference area and mean aerodynamic chord, respectively.

The atmospheric force and moment coefficients are given by

$$C_T = c_{T0} + c_T^{\beta}\beta \tag{11}$$

$$C_D = c_{D0} + c_D^{\alpha}\alpha + c_D^{\alpha^2}\alpha^2 \tag{12}$$

$$C_L = c_L^{\alpha}\alpha \tag{13}$$

$$C_{m_z} = m_{z0} + m_z^{\alpha}\alpha + m_z^{\alpha^2}\alpha^2 + m_z^{\omega_z}\omega_z + m_z^{\delta_e}\delta_e \tag{14}$$

where β is the throttle setting, δ_e is the elevator deflection angle.

In addition, the second-order engine dynamics can be described as

$$\ddot{\beta} = -2\xi\omega_n\dot{\beta} - \omega_n^2\beta + \omega_n^2\beta_c + d_7, \tag{15}$$

where β_c is the demand of throttle setting, ξ is the damping ratio of the engine dynamics, ω_n is the undamped natural frequency, d_7 is the external disturbance of the throttle.

Remark 1: In fact, the disturbances of $\dot{h}$, $\dot{\vartheta}$ and $\dot{\beta}$ are not concerned in this study for the reason of their accurate mathematics deduction. Besides, the disturbance terms d_i, $i = 2, 4, 5, 7$, can be regarded as the equivalent disturbances consisting of external disturbances, internal uncertainties and model errors which can be well tackled by the disturbance observers.

B. MODEL TRANSFORMATION

In the process of controller designing, the AHV system is required to be expressed in the strict feedback formulations. Before the model transformation, following assumptions are introduced.

Assumption 1 [26], [29], [40]: The thrust term $T\sin\alpha$ in (2) can be omitted, since it is commonly much smaller than L.

Assumption 2 [26], [29], [40]: The flight path angle θ maintains a small value, which means $\sin\theta \approx \theta$.

To depict the AHV longitudinal model (1)-(6) and (15) more explicitly, the system states and the control inputs are defined as $x_1 = h, x_2 = \theta, x_3 = \vartheta, x_4 = \omega_z, x_5 = V, x_6 = \beta, x_7 = \dot{\beta}, u_1 = \delta_e, u_2 = \beta_c$, respectively.

Thus, considering Assumption 1 and 2, the AHV longitudinal system can be divided into the altitude subsystem and the velocity subsystem as follows.

$$\begin{aligned}
\dot{x}_1 &= g_1 x_2, \\
\dot{x}_2 &= g_2 x_3 + f_2 + d_2, \\
\dot{x}_3 &= g_3 x_4, \\
\dot{x}_4 &= g_4 u_1 + f_4 + d_4, \\
\dot{x}_5 &= g_5 x_6 + f_5 + d_5 \\
\dot{x}_6 &= g_6 x_7 \\
\dot{x}_7 &= g_7 u_2 + f_7 + d_7
\end{aligned} \tag{16}$$

$$\tag{17}$$

where f_j, $j = 2, 4, 5, 7$, and g_i, $i = 1, 2, \ldots, 7$, represent the dynamics of relevant channels for AHV longitudinal model

which can be expressed as

$$
\begin{aligned}
&g_1 = x_5,\ g_2 = \frac{c_L^{\alpha}\rho S x_5}{2m},\\
&f_2 = -\frac{(\mu - x_5^2(x_1+R_E))\cos x_2}{x_5^2(x_1+R_E)^2} - g_2 x_2,\\
&g_3 = 1,\ g_4 = \frac{m_z^{\delta_e}\rho S l x_5^2}{2J_z},\\
&f_4 = \frac{\rho S l x_5^2}{2J_z}(m_{z0} + m_z^{\alpha}(x_3 - x_2) + m_z^{\alpha^2}(x_3 - x_2)^2\\
&\quad + m_z^{\omega_z} x_4),\\
&g_5 = \frac{c_T^{\beta}\rho S x_5^2 \cos(x_3 - x_2)}{2m},\\
&f_5 = -\frac{\rho S x_5^2}{2m}(c_{D0} + c_D^{\alpha}(x_3 - x_2) + c_D^{\alpha^2}(x_3 - x_2)^2)\\
&\quad + \frac{c_{T0}\rho S x_5^2 \cos(x_3 - x_2)}{2m} - \frac{\mu \sin x_2}{(x_1 + R_E)^2},\\
&g_6 = 1, \quad g_7 = \omega_n^2,\ f_7 = -2\xi\omega_n x_7 - \omega_n^2 x_6.
\end{aligned} \tag{18}
$$

Assumption 3 [37], [47]: The functions g_i, $i = 1, 2, \ldots, 7$, satisfy $|g_i| < \bar{g}_i$, where $\bar{g}_i > 0$.

This assumption can ensure that the control inputs are nonsingular and bounded.

III. SMOOTH SUPER TWISTING ALGORITHM BASED DISTURBANCE OBSERVER DESIGN

In this section, the smooth super twisting algorithm based disturbance observer (SSTDOB) is developed for the AHV system, which can compensate the equivalent disturbances. Besides, the convergence time of the disturbance observation error is also analyzed.

A. OBSERVER DESIGN

It is shown that disturbances $d_i, i = 2, 4, 5, 7$, are respectively involved in the differential equation for x_2, x_4, x_5 and x_7 without couplings. Thus, observer for d_i can be designed independently. Before the design of this SSTDOB, the following assumption is made.

Assumption 4: [26], [29], [40] The disturbances d_i, $i = 2, 4, 5, 7$, are considered to be bounded, that is to say $|d_i| \le \bar{d}_i$, $|\dot{d}_i| \le \delta_i$, where $\bar{d}_i > 0$ and $\delta_i \ge 0$.

Considering the observer for d_i, the relevant auxiliary variables y_i, $i = 2, 4, 5, 7$, can be constructed as

$$\dot{y}_i = \psi_i + \hat{d}_i \tag{19}$$

where ψ_i can be expressed as

$$\psi_i = \begin{cases} g_2 x_3 + f_2 & i = 2 \\ g_4 u_1 + f_4 & i = 4 \\ g_5 x_6 + f_5 & i = 5 \\ g_7 u_2 + f_7 & i = 7 \end{cases} \tag{20}$$

Errors between x_i and y_i are defined as $e_{i1} = x_i - y_i$. With the assistance of e_{i1}, observer for d_i can be designed as

$$
\begin{aligned}
\hat{d}_i = {} & k_{i1}\mathrm{sig}(e_{i1})^{\frac{p_i-1}{p_i}} + k_{i2}e_{i1}\\
& + \int_0^t \left(k_{i3}\mathrm{sig}\,(e_{i1}(\tau))^{\frac{p_i-2}{p_i}} + k_{i4}e_{i1}(\tau)\right)d\tau
\end{aligned} \tag{21}
$$

In (21), k_{i1}, k_{i2}, k_{i3}, k_{i4} and $p_i, i = 2, 4, 5, 7$ are all positive constants and satisfy following conditions

$$\begin{cases} p_i \ge 2, & k_{i1} > 2\sqrt{\delta_i}, \quad k_{i2} > 0, \\ k_{i3} > \delta_i, & k_{i4} > k_{i4}^{\Omega} \end{cases} \tag{22}$$

where $k_{i4}^{\Omega} = \frac{(\frac{p_i-1}{p_i}k_{i1}k_{i2}+k_{i1}k_{i2})^2(\frac{p_i-1}{p_i}(k_{i1}^2+4k_{i3})-(k_{i3}-\delta_i))}{N_i} - \frac{p_i-1}{p_i}k_{i2}^2 - 2k_{i2}^2$ with $N_i = (\frac{p_i-1}{pi}(k_{i1}^4 + 4k_{i1}^2k_{i3}) - k_{i1}^2(k_{i3} - \delta_i))(\frac{p_i-1}{pi}(-k_{i1}^2 - 2k_{i3}) + (k_{i3} - \delta_i))$.

B. STABILITY ANALYZATION FOR SSTDOB

With Assumption 4, the following Theorem 1 of proposed SSTDOB for AHV can be established.

Theorem 1: With the proposed SSTDOB (21), observation errors of x_i, $i = 2, 4, 5, 7$, can converge to 0 in finite time.

Proof: Combining (19) and the differential equations for $x_i, i = 2, 4, 5, 7$, in (16) and (17), it can be easily acquired that

$$\dot{e}_{i1} = d_i - \hat{d}_i \tag{23}$$

Substituting (21) into (23), we have

$$
\begin{aligned}
\dot{e}_{i1} = {} & d_i - k_{i1}\mathrm{sig}\,(e_{i1})^{\frac{p_i-1}{p_i}} - k_{i2}e_{i1}\\
& - \int_0^t \left(k_{i3}\mathrm{sig}\,(e_{i1}(\tau))^{\frac{p_i-2}{p_i}} + k_{i4}e_{i1}(\tau)\right)d\tau
\end{aligned} \tag{24}
$$

To facilitate the following deduction, we define $e_{i2} = d_i - \int_0^t \left(k_{i3}\mathrm{sig}\,(e_{i1}(\tau))^{\frac{p_i-2}{p_i}} + k_{i4}e_{i1}(\tau)\right)d\tau$. Evidently, (24) can be reformed as the following second-order system.

$$\begin{cases} \dot{e}_{i1} = -k_{i1}\mathrm{sig}\,(e_{i1})^{\frac{p_i-1}{p_i}} - k_{i2}e_{i1} + e_{i2} \\ \dot{e}_{i2} = -k_{i3}\mathrm{sig}\,(e_{i1})^{\frac{p_i-2}{p_i}} - k_{i4}e_{i1} + \dot{d}_i \end{cases} \tag{25}$$

Consider the Lyapunov candidate function

$$
\begin{aligned}
V_i = {} & 2k_{i3}|e_{i1}|^{\frac{2p_i-2}{p_i}} + k_{i4}e_{i1}^2 + \frac{1}{2}e_{i2}^2\\
& + \frac{1}{2}\left(k_{i1}\mathrm{sig}\,(e_{i1})^{\frac{p_i-1}{p_i}} + k_{i2}e_{i1} - e_{i2}\right)^2\\
= {} & \xi_i^T P_i \xi_i \le \lambda_{\max}(P_i)\,\|\xi_i\|_2^2
\end{aligned} \tag{26}
$$

where

$$\xi_i = \begin{bmatrix} \mathrm{sig}\,(e_{i1})^{\frac{p_i-1}{p_i}} \\ e_{i1} \\ e_{i2} \end{bmatrix} \tag{27}$$

$$P_i = \begin{bmatrix} 2k_{i3} + \frac{1}{2}k_{i1}^2 & \frac{1}{2}k_{i1}k_{i2} & -\frac{1}{2}k_{i1} \\ \frac{1}{2}k_{i1}k_{i2} & k_{i4} + \frac{1}{2}k_{i2}^2 & -\frac{1}{2}k_{i2} \\ -\frac{1}{2}k_{i1} & -\frac{1}{2}k_{i2} & 1 \end{bmatrix} \tag{28}$$

We note that the derivative of ξ_i can be expressed as

$$\begin{aligned}\dot{\xi}_i &= \begin{bmatrix} \frac{p_i-1}{p_i}|e_{i1}|^{-\frac{1}{p_i}}\dot{e}_{i1} \\ \dot{e}_{i1} \\ \dot{e}_{i2} \end{bmatrix} \\ &= \begin{bmatrix} \frac{p_i-1}{p_i}|e_{i1}|^{-\frac{1}{p_i}}\left(-k_{i1}\mathrm{sig}\,(e_{i1})^{\frac{p_i-1}{p_i}} - k_{i2}e_{i1} + e_{i2}\right) \\ -k_{i1}\mathrm{sig}\,(e_{i1})^{\frac{p_i-1}{p_i}} - k_{i2}e_{i1} + e_{i2} \\ -k_{i3}\mathrm{sig}\,(e_{i1})^{\frac{p_i-2}{p_i}} - k_{i4}e_{i1} + \dot{d}_i \end{bmatrix} \\ &= |e_{i1}|^{-\frac{1}{p_i}}A_i\xi_i + B_i\xi_i + \begin{bmatrix} 0 \\ 0 \\ \dot{d}_i \end{bmatrix} \end{aligned} \tag{29}$$

where

$$A_i = \begin{bmatrix} -\frac{p_i-1}{p_i}k_{i1} & -\frac{p_i-1}{p_i}k_{i2} & \frac{p_i-1}{p_i} \\ 0 & 0 & 0 \\ -k_{i3} & 0 & 0 \end{bmatrix}$$

$$B_i = \begin{bmatrix} 0 & 0 & 0 \\ -k_{i1} & -k_{i2} & 1 \\ 0 & -k_{i4} & 0 \end{bmatrix}$$

Using Assumption 4 and setting $\kappa_i(t) = \mathrm{sign}\,(e_{i1})|e_{i1}|^{\frac{2-p_i}{p_i}}\dot{d}_i$, the time derivative of V_i can become

$$\begin{aligned}\dot{V}_i &= \dot{\xi}_i^T P_i\xi_i + \xi_i^T P_i\dot{\xi}_i \\ &= |e_{i1}|^{-\frac{1}{p_i}}\xi_i^T\left(P_iA_i + A_i^TP_i\right)\xi_i + \xi_i^T\left(P_iB_i + B_i^TP_i\right)\xi_i \\ &\quad + 2|e_{i1}|^{-\frac{1}{p_i}}\begin{bmatrix} 0 & 0 & |e_{i1}|^{\frac{1}{p_i}}\dot{d} \end{bmatrix}P_i\xi_i^T \\ &= |e_{i1}|^{-\frac{1}{p_i}}\xi_i^T\left(P_iA_i + A_i^TP_i\right)\xi_i + \xi_i^T\left(P_iB_i + B_i^TP_i\right)\xi_i \\ &\quad + |e_{i1}|^{-\frac{1}{p_i}}\xi_i^T\left(P_iM_i(t) + M_i(t)^TP_i\right)\xi_i \\ &= |e_{i1}|^{-\frac{1}{p_i}}\xi_i^T\left(P_i(A_i + M_i(t)) + (A_i + M_i(t))^TP_i\right)\xi_i \\ &\quad + \xi_i^T\left(P_iB_i + B_i^TP_i\right)\xi_i \\ &= -|e_{i1}|^{-\frac{1}{p_i}}\xi_i^TQ_i\xi_i - \xi_i^TR_i\xi_i \end{aligned} \tag{30}$$

where

$$M_i(t) = \begin{bmatrix} 0 & 0 & 0 \\ 0 & 0 & 0 \\ \kappa_i(t) & 0 & 0 \end{bmatrix} \tag{31}$$

$$Q_i = \begin{bmatrix} Q_{11} & Q_{12} & Q_{13} \\ Q_{21} & Q_{22} & Q_{23} \\ Q_{31} & Q_{32} & Q_{33} \end{bmatrix} \tag{32}$$

$$R_i = \begin{bmatrix} R_{11} & R_{12} & R_{13} \\ R_{21} & R_{22} & R_{23} \\ R_{31} & R_{32} & R_{33} \end{bmatrix} \tag{33}$$

with their elements

$$\begin{aligned} Q_{11} &= \frac{p_i-1}{p_i}\left(k_{i1}^3 + 4k_{i1}k_{i3}\right) - k_{i1}(k_{i3} - \kappa_i(t)), \\ Q_{12} &= \frac{p_i-1}{p}(2k_{i2}k_{i3} + k_{i1}^2k_{i2}) - \frac{1}{2}k_{i2}(k_{i3} - \kappa_i(t)), \\ Q_{13} &= -\frac{p_i-1}{p_i}(k_{i1}^2 + 2k_{i3}) + (k_i3 - \kappa_i(t)), \\ Q_{22} &= \frac{p_i-1}{p_i}k_{i1}k_{i2}^2, \quad Q_{23} = -\frac{p_i-1}{p_i}k_{i1}k_{i2}, \\ Q_{21} &= Q_{12}, \quad Q_{31} = Q_{13}, \; Q_{32} = Q_{23}, \\ Q_{33} &= \frac{p_i-1}{p_i}k_{i1}, \\ R_{11} &= k_{i1}^2k_{i2}, \quad R_{12} = k_{i1}k_{i2}^2 + \frac{1}{2}k_{i1}k_{i4}, \\ R_{13} &= -k_{i1}k_{i2}, \quad R_{22} = k_{i2}^3 + k_{i2}k_{i4}, \\ R_{23} &= k_{i2}^2, \quad R_{33} = k_{i2}, \\ R_{21} &= R_{12}, \quad R_{31} = R_{13}, \; R_{32} = R_{23} \end{aligned}$$

Obviously, the following relations hold.

$$\mathrm{sig}\,(e_{i1})^{\frac{p_i-1}{p_i}} \cdot e_{i1} = |e_{i1}|^{-\frac{1}{p_i}} \cdot e_{i1}^2 \tag{34}$$

$$\mathrm{sig}\,(e_{i1})^{\frac{p_i-1}{p_i}} \cdot e_{i2} = |e_{i1}|^{-\frac{1}{p_i}} \cdot e_{i1} \cdot e_{i2} \tag{35}$$

$$|e_{i1}|^{-\frac{1}{p_i}} \cdot \mathrm{sig}\,(e_{i1})^{\frac{p_i-1}{p_i}} \cdot e_{i1} = \mathrm{sig}\,(e_{i1})^{\frac{2(p_i-1)}{p_i}} \tag{36}$$

Thus, substituting (34)-(36) into (30), we have

$$\dot{V}_i = -|e_{i1}|^{-\frac{1}{p_i}}\xi_i^T\bar{Q}_i\xi_i - \xi_i^T\bar{R}_i\xi_i \tag{37}$$

where

$$\bar{Q}_i = \begin{bmatrix} Q_{11} & 0 & Q_{13} \\ 0 & Q_{22} - 2R_{12} & Q_{23} + R_{13} \\ Q_{31} & Q_{32} + R_{31} & Q_{33} \end{bmatrix} \tag{38}$$

$$\bar{R}_i = \begin{bmatrix} R_{11} - 2Q_{12} & 0 & 0 \\ 0 & R_{22} & R_{23} \\ 0 & R_{32} & R_{33} \end{bmatrix} \tag{39}$$

Due to the fact that $k_{ij}, i = 2, 4, 5, 7, j = 1, 2, 3, 4$ are all positive constants with conditions (22) hold, $\bar{Q}_i$ and $\bar{R}_i$ are all positive definite matrices. Therefore, (37) can be reformed as

$$\begin{aligned}\dot{V}_i &\le -\lambda_{\min}\left(\bar{Q}_i\right)|e_{i1}|^{-\frac{1}{p_i}}\|\xi_i\|_2^2 - \lambda_{\min}\left(\bar{R}_i\right)\|\xi_i\|_2^2 \\ &= -\lambda_{\min}\left(\bar{Q}_i\right)\left(|e_{i1}|^{\frac{p_i-1}{p_i}}\right)^{-\frac{1}{p_i-1}}\|\xi_i\|_2^2 - \lambda_{\min}\left(\bar{R}_i\right)\|\xi_i\|_2^2 \\ &\le -\lambda_{\min}\left(\bar{Q}_i\right)\|\xi_i\|_2^{-\frac{1}{p_i-1}}\|\xi_i\|_2^2 - \lambda_{\min}\left(\bar{R}_i\right)\|\xi_i\|_2^2 \\ &= -\lambda_{\min}\left(\bar{Q}_i\right)\|\xi_i\|_2^{\frac{2p_i-3}{p_i-1}} - \lambda_{\min}\left(\bar{R}_i\right)\|\xi_i\|_2^2 \end{aligned} \tag{40}$$

Combining (26) and (40), it can be acquired that

$$\dot{V}_i + \alpha_iV_i^{\gamma_i} + \beta_iV_i \le 0 \tag{41}$$

where $\alpha_i = \frac{\lambda_{\min}(\bar{Q}_i)}{\lambda_{\max}(P_i)^{\frac{2p_i-3}{2p_i-2}}}$, $\gamma_i = \frac{2p_i-3}{2p_i-2}$, $\beta_i = \frac{\lambda_{\min}(\bar{R}_i)}{\lambda_{\max}(P_i)}$, $i = 2, 4, 5, 7$.

Thus, according to Yu *et al.* [46], V_i will converge to 0 in finite time, that is, e_{i1} and e_{i2} converge to 0 in finite time.

In addition, the convergence time t_i can be evaluated by

$$t_i = \int_{V_i(0)}^{0} \frac{1}{\dot{V}_i} dV_i \le \int_0^{V_i(0)} \frac{1}{\alpha_i V_i^{\gamma_i} + \beta_i V_i} dV_i = \frac{1}{\beta_i (1-\gamma_i)} \ln \frac{\beta_i V_i(0)^{1-\gamma_i} + \alpha_i}{\alpha_i} \tag{42}$$

Since $(e_{i1} = 0, e_{i2} = 0)$ is the equilibrium point of (25), $e_{i1}(t) = 0$ is satisfied for all $t > t_i$, which indicates that $\dot{e}_{i1}(t) = 0$ for any $t > t_i$. According to (23), it can be obtained that

$$\tilde{d}_i(t) = d_i(t) - \hat{d}_i(t) = 0, \forall t > t_i \tag{43}$$

Therefore, observation errors of d_i, $i = 2, 4, 5, 7$, can converge to 0 in finite time, which means the equivalent disturbances can be exactly estimated in finite time. The proof of SSTDOB's stability is complete.

Remark 2: When $\delta_i = 0, i = 2, 4, 5, 7, p_i$ can be chosen as $p_i \ge 2$, then the disturbance observation errors can converge to the origin in finite time. When $\delta_i > 0$, two cases can be discussed.

Case A: $0 < \delta_i < \varsigma_i$, where the terms ς_i are small enough positive constants. This indicates that the disturbances are slow varying, that is, $\dot{d}_i \approx 0$. Then, (29) becomes

$$\dot{x}_i \approx |e_{i1}|^{-\frac{1}{p_i}} A_i \xi_i + B_i \xi_i \tag{44}$$

The finite time stability of proposed SSTDOB won't rely on the boundedness of $\kappa_i(t)$. Therefore, the disturbance observer can still work well when $0 < \delta_i < \varsigma_i$ and $p_i \ge 2$.

Case B: $\delta_i \ge \varsigma_i$. In this situation, the disturbances have higher frequency or larger amplitude. The finite time stability of proposed SSTDOB will depend on the boundedness of $\kappa_i(t)$. Then, setting $p_i = 2$, we yield

$$|\kappa_i(t)| = \left|\text{sign}(e_{i1})\dot{d}_i\right| \le \delta_i \tag{45}$$

With (45), the boundedness of $\kappa_i(t)$ can be guaranteed, which will maintain the finite time performance of the observer. Accordingly, the newly proposed observer will revert to the following equation [48]

$$\hat{d}_i = k_{i1} \text{sig}(e_{i1})^{\frac{1}{2}} + k_{i2} e_{i1} + \int_0^t \left(k_{i3} \text{sign}(e_{i1}(\tau)) + k_{i4} e_{i1}(\tau)\right) d\tau \tag{46}$$

Therefore, case A will explain the simulation results with slow varying disturbances, that is, $0 < \delta_i < \varsigma_i$ and $p_i \ge 2$. Compared with super twisting algorithm-based observer designed in Nagesh and Edwards [48], the selection of p_i are more flexible, which means that this SSTDOB have more generic formulation for slow varying disturbance estimation. Besides, it will be illustrated that the proposed SSTDOB can achieve excellent estimation ability if we choose $p_i = 2$ for both case A and case B.

Remark 3: As mentioned in Nagesh and Edwards [48], the Filippov solution of (21) cannot stay on $(e_{i1} = 0, e_{i2} = 0)$. There exists some small time interval T_o containing t_i e_{i1} will monotonically pass through zero. Therefore, (40) holds almost everywhere and the observer will converge to the equilibrium point $(e_{i1} = 0, e_{i2} = 0)$ in finite time.

Remark 4: Since the possible discontinuous function $\text{sig}(e_{i1})^{\frac{p_i-2}{p_i}}$ is hidden in the integral item, $\hat{d}_i$ will be continuous (non-Lipschitzian) and the chattering is eliminated. Besides, calculating the derivative of $\hat{d}_i$ we can yield

$$\dot{\hat{d}}_i = k_{i1} \frac{p_i - 1}{p_i} \text{sign}(e_{i1})^{-\frac{1}{p_i}} \dot{e}_{i1} + k_{i2} \dot{e}_{i1} + k_{i3} \text{sig}(e_{i1})^{\frac{p_i-2}{p_i}} + k_{i4} e_{i1} \tag{47}$$

With (25), it is apparent that $e_{i1}, e_{i2}, \dot{e}_{i1}$ and $\text{sig}(e_{i1})^{\frac{p_i-2}{p_i}}$ are continuous. Thus, the continuity of (47) will depend on the terms $\Theta_i = \text{sign}(e_{i1})^{-\frac{1}{p_i}} \dot{e}_{i1}$. Substituting the first formula of (25) into Θ_i, we have

$$\Theta_i = -k_{i1} \text{sign}(e_{i1})^{\frac{p_i-1}{p_i}} |e_{i1}|^{\frac{p_i-1}{p_i}} - k_{i2} \text{sign}(e_{i1})^{-\frac{1}{p_i}} e_{i1} + \text{sign}(e_{i1})^{-\frac{1}{p_i}} e_{i2} \tag{48}$$

When $e_{i1} \to 0^+$, we have $\lim_{e_{i1} \to 0^+} = 0$; when $e_{i1} \to 0^-$, we have $\lim_{e_{i1} \to 0^-} = 0$. Therefore, Θ_i is continuous and it follows that $\dot{\hat{d}}_i$ is continuous. Finally, the smoothness of $\hat{d}_i$ can be guaranteed. Besides, it will be illustrated in the simulation results that the proposed SSTDOB can exhibit smoother outputs.

Remark 5: When e_{i1} and e_{i2} converge to zero after finite time t_i, (25) becomes

$$\begin{cases} \dot{e}_{i1} = e_{i2} = 0 \\ \dot{e}_{i2} = \dot{d}_i \end{cases} \tag{49}$$

With the first formula of (49) and (23), we can make a conclusion that the observation errors of d_i will also converge to zero. As for the second formula of (49), the following inequality holds

$$|\dot{e}_{i2}| = \left|\dot{d}_i\right| \le \delta_i \tag{50}$$

Therefore, the result of (50) is consistent with the boundedness of $\dot{d}_i$ in Assumption 4.

IV. SSTDOB BASED FSMBC FOR AHV SYSTEM

The main objective of this paper is to design a good performance of controller which can track the desired altitude x_{1d} and desired velocity x_{5d} respectively. Thus, the SSTDOB based fixed-time sliding mode backstepping control (FSMBC) strategy is proposed for the AHV longitudinal system. The block diagram of this composite controller is shown in Figure 2.

Before the controller designing, some lemmas and assumptions are given as follows

Lemma 1 [37], [47], [49]: Consider a scalar system is expressed as follow

$$\dot{y} = -a \text{sig}(y)^{\alpha} - b \text{sig}(y)^{\beta}, y(0) = y_0 \tag{51}$$

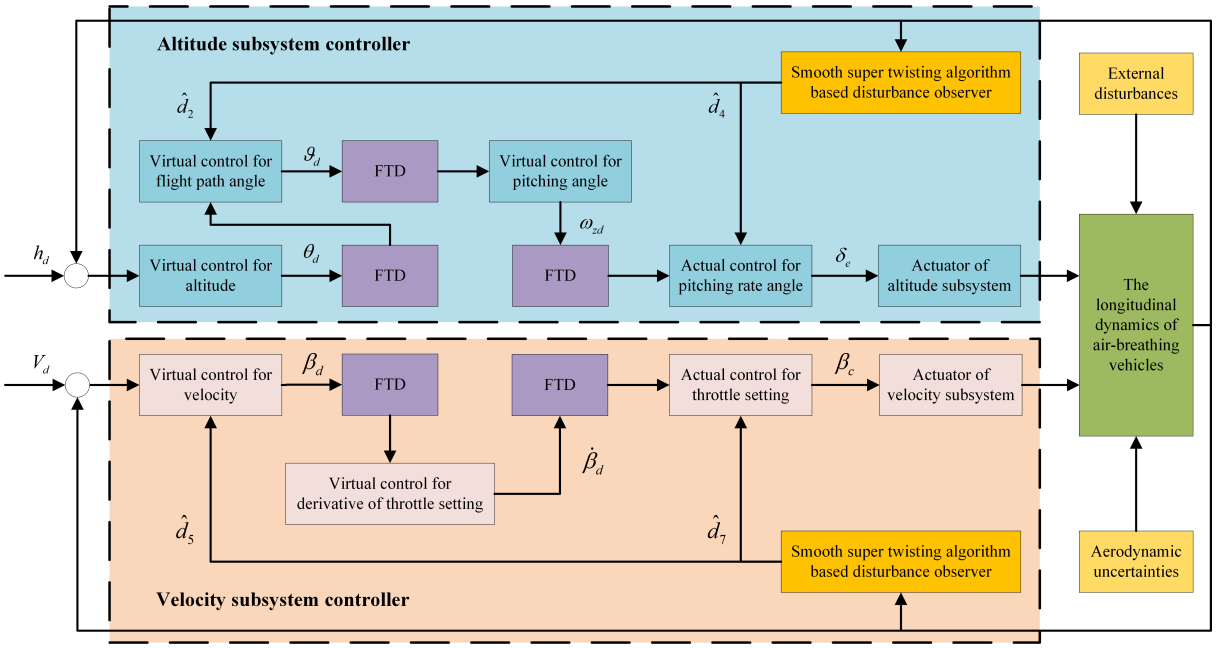

FIGURE 2. The block diagram of proposed composite controller.

where $a > 0, b > 0, \alpha > 1, 0 < \beta < 1$. System (51) has globally fixed-time stability with convergence time T bounded by

$$T \leq \frac{1}{a}\frac{1}{\alpha-1} + \frac{1}{b}\frac{1}{1-\beta} \tag{52}$$

Besides, when system (51) becomes

$$\dot{y} = -a\mathrm{sig}(y)^{\alpha} - b\mathrm{sig}(y)^{\beta} + \Phi, y(0) = y_0 \tag{53}$$

where Φ is a small positive real number. Then the system (53) will converge to an arbitrarily small neighbor of the origin, i.e. $y \leq 2\Pi$ with $\Phi = a\mathrm{sig}(\Pi)^{\alpha} + b\mathrm{sig}(\Pi)^{\beta}$, within a fixed-time bounded by

$$T < \frac{1}{a}\frac{1}{\alpha-1} + \frac{1}{b(2^{\beta}-1)}\frac{1}{1-\beta} \tag{54}$$

Lemma 2 [37], [47], [49]: For $\xi_1, \xi_2, \ldots, \xi_n \geq 0$ and $p > 0$, the following inequality can hold

$$\max(n^{p-1}, 1)(\xi_1^p + \xi_2^p + \cdots + \xi_n^p) \geq (\xi_1 + \xi_2 + \cdots + \xi_n)^p \tag{55}$$

Lemma 3 [45]: Consider the differentiators are expressed as

$$\begin{cases} \dot{\sigma}_{i1} = \sigma_{i2} - \lambda_{i1}\mathrm{sig}(\sigma_{i1} - x_{id})^{\alpha_i} - \kappa_{i1}\mathrm{sig}(\sigma_{i1} - x_{id})^{\beta_i} \\ \dot{\sigma}_{i2} = -\lambda_{i2}\mathrm{sig}(\sigma_{i1} - x_{id})^{\bar{\alpha}_i} - \kappa_{i2}\mathrm{sig}(\sigma_{i1} - x_{id})^{\bar{\beta}_i} \end{cases} \tag{56}$$

where $e_i = \sigma_{i1} - x_{id}, i = 2, 3, 4, 6, 7$, σ_{i1} and σ_{i2} are the estimation of x_{id} and $\dot{x}_{id}$, respectively. $\alpha_i > 1$, $0 < \beta_i < 1$, $\bar{\alpha}_i = 2\alpha_i - 1$, $\bar{\beta}_i = 2\beta_i - 1$, $\lambda_{i1}, \lambda_{i2}, \kappa_{i1}$ and κ_{i2} are positive constants such that the matrices $\tilde{A}_{i1}$ and $\tilde{A}_i$ are Hurwitz.

$$\tilde{A}_{i1} = \begin{bmatrix} -\lambda_{i1} & 1 \\ -\lambda_{i2} & 0 \end{bmatrix} \tag{57}$$

$$\tilde{A}_i = \begin{bmatrix} -\kappa_{i1} & 1 \\ -\kappa_{i2} & 0 \end{bmatrix} \tag{58}$$

With (56) satisfying above conditions, the errors e_i can converge to the origin and σ_{i2} will converge to the derivative of virtual control x_{id} in a fixed-time bounded by

$$t_{FTDi} \leq \frac{\lambda_{\max}\left(\tilde{P}_{i1}\right)}{\lambda_{\min}\left(\tilde{Q}_{i1}\right)(\alpha_i - 1)\,\Gamma^{\alpha_i - 1}} + \frac{\lambda_{\max}^{2-\beta_i}\left(\tilde{P}_i\right)}{\lambda_{\min}\left(Q_i\right)(1-\beta_i)} \tag{59}$$

where $0 < \Gamma \leq \lambda_{\min}(\tilde{P}_{i1})$, the symmetric positive matrices $\tilde{P}_{i1}$ and $\tilde{Q}_{i1}$ satisfy

$$\tilde{P}_{i1}\tilde{A}_{i1} + \tilde{A}_{i1}^T\tilde{P}_{i1} = -\tilde{Q}_{i1} \tag{60}$$

The symmetric positive matrices $\tilde{P}_i$ and $\tilde{Q}_i$ satisfy

$$\tilde{P}_i\tilde{A}_i + \tilde{A}_i^T\tilde{P}_i = -\tilde{Q}_i \tag{61}$$

Remark 6: According to Lemma 3, when $t > t_{FTDi}$, the fixed-time tracking differentiator (FTD) (56) will exhibit an exact estimation of x_{id} and $\dot{x}_{id}$,that is,

$$\begin{cases} e_i = 0 \\ \dot{e}_i = 0 \end{cases} \Rightarrow \begin{cases} x_{id} = \sigma_{i1} \\ \dot{x}_{id} = \dot{\sigma}_{i1} = \sigma_{i2} \end{cases} \tag{62}$$

Assumption 5 [40]: The initial tracking errors $z_i(0)$, $i = 1, 2, \ldots, 7$, are bounded satisfying

$$z_i(0) \leq |z_i(0)| < \eta_i \quad (i = 1, 2, \ldots, 7) \tag{63}$$

where $\eta_1, \eta_2, \ldots, \eta_7$ are positive constants.

A. SSTDOB-FSMBC DESIGN FOR ALTITUDE SUBSYSTEM

Step 1.1 (virtual control input for altitude): Define the tracking error of altitude x_1 as $z_1 = x_1 - x_{1d}$. Then we select a sliding surface

$$s_1 = l_1 \left(z_1 - z_1 \left(0\right) \exp\left(-\varphi_1 t\right)\right) \tag{64}$$

where $l_1 \geq 1$, $\varphi_1 > 0$, $z_1(0)$ is the initial error of x_1.

Computing the time derivative of (64) we yield

$$\dot{s}_1 = l_1 \left(g_1 x_2 - \dot{x}_{1d} + \varphi_1 z_1 \left(0\right) \exp\left(-\varphi_1 t\right)\right) \tag{65}$$

Thus, the virtual control input x_{2d} adopted by backstepping control can be given as

$$x_{2d} = -\frac{1}{g_1}(-\dot{x}_{1d} + \varphi_1 z_1 \left(0\right) \exp\left(-\varphi_1 t\right) + a_1 \mathrm{sig}(s_1)^{\alpha_1} + b_1 F_1(s_1) + c_1 s_1) \tag{66}$$

where a_1, b_1 and c_1 are positive constants, $\alpha_1 > 1$. $F_1(s_1)$ is constructed as

$$F_1(s_1) = \begin{cases} \mathrm{sig}(s_1)^{\beta_1}, & |s_1| \geq \varepsilon_1 \\ \tau_{11} s_1 + \tau_{12} s_1^2 \mathrm{sign}\left(s_1\right), & |s_1| < \varepsilon_1 \end{cases} \tag{67}$$

where $0 < \beta_1 < 1$, ε_1 is a small enough positive constant, $\tau_{11} = (2 - \beta_1)\, \varepsilon_1^{\beta_1 - 1}$, $\tau_{12} = (\beta_1 - 1)\, \varepsilon_1^{\beta_1 - 2}$.

To avoid the "explosion of complexity" involved in control law, a fixed-time tracking differentiator (FTD) is introduced as

$$\begin{cases} \dot{\sigma}_{21} = \sigma_{22} - \lambda_{21} \mathrm{sig}(\sigma_{21} - x_{2d})^{\alpha_2} - \kappa_{21} \mathrm{sig}(\sigma_{21} - x_{2d})^{\beta_2} \\ \dot{\sigma}_{22} = -\lambda_{22} \mathrm{sig}(\sigma_{21} - x_{2d})^{\bar{\alpha}_2} - \kappa_{i2} \mathrm{sig}(\sigma_{21} - x_{2d})^{\bar{\beta}_2} \end{cases} \tag{68}$$

where $\alpha_2 > 1$, $0 < \beta_2 < 1$, $\bar{\alpha}_2 = 2\alpha_2 - 1$, $\bar{\beta}_2 = 2\beta_2 - 1$. The selection conditions of λ_{21}, λ_{22}, κ_{21} and κ_{22} are same to Lemma 3.

Define $z_2 = x_2 - \sigma_{21}$, $e_2 = \sigma_{21} - x_{2d}$, (65) becomes

$$\begin{aligned} \dot{s}_1 &= l_1 \left(g_1 \left(z_2 + e_2 + x_{2d}\right) - \dot{x}_{1d} + \varphi_1 z_1 \left(0\right) \exp\left(-\varphi_1 t\right)\right) \\ &= l_1 (g_1 z_2 + g_1 e_2 - a_1 \mathrm{sig}(s_1)^{\alpha_1} - b_1 F_1(s_1) - c_1 s_1) \end{aligned} \tag{69}$$

Remark 7: Inspired by Zhou *et al.* [49], we introduce this switching logic in $F_1(s_1)$ to avoid the singularity problem in $\dot{x}_{2d}$. When $|s_1| \geq \varepsilon_1$ calculating the derivative of x_{2d} yields the term $\dot{F}_1(s_1) = \beta_1 |s_1|^{\beta_1 - 1} \dot{s}_1$. Since $|s_1| \geq \varepsilon_1 > 0$, the singularity problem cannot appear in this situation. When $|s_1| < \varepsilon_1$, calculating the derivative of x_{2d}, we have the term $\dot{F}_1(s_1) = \tau_{11} \dot{s}_1 + 2\tau_{12} |s_1| \dot{s}_1$. It is apparent that this term will not turn to singular when $s = 0$ and $\dot{s} \neq 0$. However, the switching effect from $\mathrm{sig}(s_1)^{\beta_1}$ to $\tau_{11} s_1 + \tau_{12} s_1^2 \mathrm{sign}(s_1)$ may degrade the fixed-time convergence property. Thus, we should select a small enough ε_1 to maintain this convergence property and avoid the singular problem. Besides, the design of τ_{11} and τ_{11} can make $F_1(s_1)$ and its derivative continuous.

Step 1.2 (virtual control input for flight path angle): The sliding surface s_2 is selected as

$$s_2 = l_2 \left(z_2 - z_2 \left(0\right) \exp\left(-\varphi_2 t\right)\right) \tag{70}$$

where $l_2 \geq 1$, $\varphi_2 > 0$, $z_2(0)$ is the initial error of x_2.

The time derivative of s_2 is

$$\dot{s}_2 = l_2 \left(g_2 x_3 + f_2 + d_2 - \dot{\sigma}_{21} + \varphi_2 z_2 \left(0\right) \exp\left(-\varphi_2 t\right)\right) \tag{71}$$

The virtual control input x_{3d} can be obtained as

$$x_{3d} = -\frac{1}{g_2}(f_2 + \hat{d}_2 - \sigma_{22} + \varphi_2 z_2 \left(0\right) \exp\left(-\varphi_2 t\right) + a_2 \mathrm{sig}(s_2)^{\alpha_2} + b_2 F_2(s_2) + c_2 s_2 + g_1 s_1) \tag{72}$$

where a_2, b_2 and c_2 are positive constants, $\alpha_2 > 1$, d_2 is estimated by SSTDOB. $F_2(s_2)$ is constructed as

$$F_2(s_2) = \begin{cases} \mathrm{sig}(s_2)^{\beta_2}, & |s_2| \geq \varepsilon_2 \\ \tau_{21} s_2 + \tau_{22} s_2^2 \mathrm{sign}\left(s_2\right), & |s_2| < \varepsilon_2 \end{cases} \tag{73}$$

where $0 < \beta_2 < 1$, ε_2 is a small enough positive constant, $\tau_{21} = (2 - \beta_2)\, \varepsilon_2^{\beta_2 - 1}$, $\tau_{22} = (\beta_2 - 1)\, \varepsilon_2^{\beta_2 - 2}$.

The FTD is designed as

$$\begin{cases} \dot{\sigma}_{31} = \sigma_{32} - \lambda_{31} \mathrm{sig}(\sigma_{31} - x_{3d})^{\alpha_3} - \kappa_{31} \mathrm{sig}(\sigma_{31} - x_{3d})^{\beta_3} \\ \dot{\sigma}_{32} = -\lambda_{32} \mathrm{sig}(\sigma_{31} - x_{3d})^{\bar{\alpha}_3} - \kappa_{32} \mathrm{sig}(\sigma_{31} - x_{3d})^{\bar{\beta}_3} \end{cases} \tag{74}$$

where the selection conditions of λ_{31}, λ_{32}, κ_{31} and κ_{32} are same to Lemma 3, $\alpha_3 > 1$, $0 < \beta_3 < 1$, $\bar{\alpha}_3 = 2\alpha_3 - 1$, $\bar{\beta}_3 = 2\beta_3 - 1$, σ_{31} is the virtual control estimated by (74).

Similarly, define $z_3 = x_3 - \sigma_{31}$, $e_3 = \sigma_{31} - x_{3d}$. Then (71) is written as

$$\begin{aligned} \dot{s}_2 &= l_2(g_2 \left(z_3 + e_3 + x_{3d}\right) + f_2 + d_2 - \dot{\sigma}_{21} + \varphi_2 z_2 \left(0\right) \exp\left(-\varphi_2 t\right)) \\ &= l_2(g_2 z_3 + g_2 e_3 + \tilde{d}_2 - a_2 \mathrm{sig}(s_2)^{\alpha_2} - b_2 F_2(s_2) - c_2 s_2 - g_1 s_1 + \sigma_{22} - \dot{\sigma}_{21}) \end{aligned} \tag{75}$$

where $\tilde{d}_2 = d_2 - \hat{d}_2$.

Step 1.3(virtual control input for pitching angle): The sliding surface s_3 and its time derivative $\dot{s}_3$ are expressed as follows

$$s_3 = l_3 \left(z_3 - z_3 \left(0\right) \exp\left(-\varphi_3 t\right)\right) \tag{76}$$

$$\dot{s}_3 = l_3 \left(x_4 - \dot{\sigma}_{31} + \varphi_3 \dot{z}_3 \left(0\right) \exp\left(-\varphi_3 t\right)\right) \tag{77}$$

where $l_3 \geq 1$, $\varphi_3 > 0$, $z_3(0)$ is the initial error of x_3.

The virtual control x_{4d} is designed as

$$x_{4d} = -\frac{1}{g_3}(-\sigma_{32} + \varphi_3 z_3 \left(0\right) \exp\left(-\varphi_3 t\right) + a_3 \mathrm{sig}(s_3)^{\alpha_3} + b_3 F_3(s_3) + c_3 s_3 + g_2 s_2)$$

with

$$F_3(s_3) = \begin{cases} \mathrm{sig}(s_3)^{\beta_3}, & |s_3| \geq \varepsilon_3 \\ \tau_{31} s_3 + \tau_{32} s_3^2 \mathrm{sign}\left(s_3\right), & |s_3| < \varepsilon_3 \end{cases} \tag{78}$$

And the FTD is expressed as

$$\begin{cases} \dot{\sigma}_{41} = \sigma_{42} - \lambda_{41}\mathrm{sig}(\sigma_{41} - x_{4d})^{\alpha_4} - \kappa_{41}\mathrm{sig}(\sigma_{41} - x_{4d})^{\beta_4} \\ \dot{\sigma}_{42} = -\lambda_{42}\mathrm{sig}(\sigma_{41} - x_{4d})^{\bar{\alpha}_4} - \kappa_{42}\mathrm{sig}(\sigma_{41} - x_{4d})^{\bar{\beta}_4} \end{cases} \tag{79}$$

In (78), (78) and (79), a_4, b_4 and c_4 are positive constants, $\alpha_3, \alpha_4 > 1$, $0 < \beta_3, \beta_4 < 1$, ε_3 is a small enough positive constant, $\tau_{31} = (2-\beta_3)\,\varepsilon_3^{\beta_3-1}$, $\tau_{32} = (\beta_3 - 1)\,\varepsilon_3^{\beta_3-2}$. The selection conditions of $\lambda_{41}, \lambda_{42}, \kappa_{41}$ and κ_{42} are same to Lemma 3, $\bar{\alpha}_4 = 2\alpha_4 - 1$, $\bar{\beta}_4 = 2\beta_4 - 1$, σ_{41} is the virtual control estimated by (74).

With the definition of $z_4 = x_4 - \sigma_{41}$ and $e_4 = \sigma_{41} - x_{4d}$, (77) becomes

$$\begin{aligned} \dot{s}_3 &= l_3\left(g_3\left(z_4 + e_4 + x_{4d}\right) - \dot{\sigma}_{31} + \varphi_3 z_3\left(0\right)\exp\left(-\varphi_3 t\right)\right) \\ &= l_3(g_3 z_4 + g_3 e_4 - a_3\mathrm{sig}(s_3)^{\alpha_3} - b_3 F_3(s_3) - c_3 s_3 \\ &\quad - g_2 s_2 + \sigma_{32} - \dot{\sigma}_{31}) \end{aligned} \tag{80}$$

Step 1.4 (Actual Control Input for Pitching Rate Angle): The sliding surface s_4 and its time derivative $\dot{s}_4$ are designed as

$$s_4 = l_4\left(z_4 - z_4\left(0\right)\exp\left(-\varphi_4 t\right)\right) \tag{81}$$

$$\dot{s}_4 = l_4\left(g_4 u_1 + f_4 + d_4 - \dot{\sigma}_{41} + \varphi_4 \dot{z}_4\left(0\right)\exp\left(-\varphi_4 t\right)\right) \tag{82}$$

where $l_4 \geq 1$, $\varphi_4 > 0$, $z_4(0)$ is the initial error of x_4.

Similar to the fore steps, the altitude subsystem actual controller u_1 can be designed as

$$\begin{aligned} u_1 = -\frac{1}{g_4}(f_4 + \hat{d}_4 - \sigma_{42} + \varphi_4 z_4\left(0\right)\exp\left(-\varphi_4 t\right) \\ + a_4\mathrm{sig}(s_4)^{\alpha_4} + b_4 F_4(s_4) + c_4 s_4 + g_3 s_3) \end{aligned} \tag{83}$$

where a_4, b_4 and c_4 are positive constants, $\alpha_4 > 1$, d_4 is estimated by SSTDOB. $F_4(s_4)$ is constructed as

$$F_4(s_4) = \begin{cases} \mathrm{sig}(s_4)^{\beta_4}, & |s_4| \geq \varepsilon_4 \\ \tau_{41} s_4 + \tau_{42} s_4^2 \mathrm{sign}\left(s_4\right), & |s_4| < \varepsilon_4 \end{cases} \tag{84}$$

where $0 < \beta_4 < 1$, ε_4 is a small enough positive constant, $\tau_{41} = (2-\beta_4)\,\varepsilon_4^{\beta_4-1}$, $\tau_{42} = (\beta_4 - 1)\,\varepsilon_4^{\beta_4-2}$.

Substituting (83) into (82), one gets

$$\begin{aligned} \dot{s}_4 = l_4(\tilde{d}_4 - a_4\mathrm{sig}(s_4)^{\alpha_4} - b_4 F_4(s_4) - c_4 s_4 \\ - g_3 s_3 + \sigma_{42} - \dot{\sigma}_{41}) \end{aligned} \tag{85}$$

where $\tilde{d}_4 = d_4 - \hat{d}_4$.

B. SSTDOB-FSMBC DESIGN FOR VELOCITY SUBSYSTEM

The design process of velocity subsystem is analogous to altitude subsystem.

Step 2.1 (virtual Control Input for Velocity): Define the velocity tracking error as $z_5 = x_5 - x_{5d}$, the sliding surface s_5 is designed as

$$s_5 = l_5\left(z_5 - z_5\left(0\right)\exp\left(-\varphi_5 t\right)\right) \tag{86}$$

where $l_5 \geq 1$, $\varphi_5 > 0$, $z_5(0)$ is the initial error of x_5.

The time derivative of s_5 is obtained as

$$\dot{s}_5 = l_5\left(g_5 x_6 + f_5 + d_5 - \dot{x}_{5d} + \varphi_5 z_5\left(0\right)\exp\left(-\varphi_5 t\right)\right) \tag{87}$$

The virtual control input x_{6d} is designed as

$$\begin{aligned} x_{6d} = -\frac{1}{g_5}(f_5 + \hat{d}_5 - \dot{x}_{5d} + \varphi_5 z_5\left(0\right)\exp\left(-\varphi_5 t\right) \\ + a_5\mathrm{sig}(s_5)^{\alpha_5} + b_5 F_5(s_5) + c_5 s_5) \end{aligned} \tag{88}$$

with

$$F_5(s_5) = \begin{cases} \mathrm{sig}(s_5)^{\beta_5}, & |s_5| \geq \varepsilon_5 \\ \tau_{51} s_5 + \tau_{52} s_5^2 \mathrm{sign}\left(s_5\right), & |s_5| < \varepsilon_5 \end{cases} \tag{89}$$

And the corresponding FTD is designed as

$$\begin{cases} \dot{\sigma}_{61} = \sigma_{62} - \lambda_{61}\mathrm{sig}(\sigma_{61} - x_{6d})^{\alpha_6} - \kappa_{61}\mathrm{sig}(\sigma_{61} - x_{6d})^{\beta_6} \\ \dot{\sigma}_{62} = -\lambda_{62}\mathrm{sig}(\sigma_{61} - x_{6d})^{\bar{\alpha}_6} - \kappa_{62}\mathrm{sig}(\sigma_{61} - x_{6d})^{\bar{\beta}_6} \end{cases} \tag{90}$$

where a_5, b_5 and c_5 are positive constants, $\alpha_5, \alpha_6 > 1$, $0 < \beta_5, \beta_6 < 1$, d_5 is estimated by SSTDOB, ε_5 is a small enough positive constant, $\tau_{61} = (2-\beta_6)\,\varepsilon_6^{\beta_6-1}$, $\tau_{62} = (\beta_6 - 1)\,\varepsilon_6^{\beta_6-2}$. The selection conditions of $\lambda_{61}, \lambda_{62}, \kappa_{61}$ and κ_{62} are also same to Lemma 3, $\bar{\alpha}_6 = 2\alpha_6 - 1$, $\bar{\beta}_6 = 2\beta_6 - 1$, σ_{61} is the virtual control estimated by (90).

Define $z_6 = x_6 - \sigma_{61}$, $e_6 = \sigma_{61} - x_{6d}$, (87) becomes

$$\begin{aligned} \dot{s}_5 &= l_5(g_5\left(z_6 + e_6 + x_{6d}\right) + f_5 + d_5 - \dot{x}_{5d} \\ &\quad + \varphi_5 z_5\left(0\right)\exp\left(-\varphi_5 t\right)) \\ &= l_5(g_5 z_6 + g_5 e_6 + \tilde{d}_5 - a_5\mathrm{sig}(s_5)^{\alpha_5} - b_5 F_5(s_5) \\ &\quad - c_5 s_5) \end{aligned} \tag{91}$$

where $\tilde{d}_5 = d_5 - \hat{d}_5$.

Step 2.2 (virtual control input for the derivative of throttle setting): Similarly, the sliding surface s_6 and its time derivative $\dot{s}_6$ are expressed as

$$s_6 = l_6\left(z_6 - z_6\left(0\right)\exp\left(-\varphi_6 t\right)\right) \tag{92}$$

$$\dot{s}_6 = l_6\left(g_6 x_7 - \dot{\sigma}_{61} + \varphi_6 z_6\left(0\right)\exp\left(-\varphi_6 t\right)\right) \tag{93}$$

where $l_6 \geq 1$, $\varphi_6 > 0$, $z_6(0)$ is the initial error of x_6.

The virtual control input x_{7d} is obtained as

$$\begin{aligned} x_{7d} = -\frac{1}{g_6}(-\sigma_{62} + \varphi_6 z_6\left(0\right)\exp\left(-\varphi_6 t\right) \\ + a_6\mathrm{sig}(s_6)^{\alpha_6} + b_6 F_6(s_6) + c_6 s_6 + g_5 s_5) \end{aligned}$$

with

$$F_6(s_6) = \begin{cases} \mathrm{sig}(s_6)^{\beta_6}, & |s_6| \geq \varepsilon_6 \\ \tau_{61} s_6 + \tau_{62} s_6^2 \mathrm{sign}\left(s_6\right), & |s_6| < \varepsilon_6 \end{cases} \tag{94}$$

And the FTD is defined as

$$\begin{cases} \dot{\sigma}_{71} = \sigma_{72} - \lambda_{71}\mathrm{sig}(\sigma_{71} - x_{7d})^{\alpha_7} - \kappa_{71}\mathrm{sig}(\sigma_{71} - x_{7d})^{\beta_7} \\ \dot{\sigma}_{72} = -\lambda_{72}\mathrm{sig}(\sigma_{71} - x_{7d})^{\bar{\alpha}_7} - \kappa_{72}\mathrm{sig}(\sigma_{71} - x_{7d})^{\bar{\beta}_7} \end{cases} \tag{95}$$

where a_6, b_6 and c_6 are positive constants, $\alpha_6, \alpha_7 > 1$, $0 < \beta_6, \beta_7 < 1$, ε_6 is a small enough positive constant,

$\tau_{71} = (2-\beta_7)\,\varepsilon_7^{\beta_7-1}$, $\tau_{72} = (\beta_7-1)\,\varepsilon_7^{\beta_7-2}$. The selection conditions of $\lambda_{71}, \lambda_{72}, \kappa_{71}$ and κ_{72} are same to Lemma 3, $\bar{\alpha}_7 = 2\alpha_7 - 1$, $\bar{\beta}_7 = 2\beta_7 - 1$, σ_{71} is the virtual control estimated by (95).

Define $z_7 = x_7 - \sigma_{71}$, $e_7 = \sigma_{71} - x_{7d}$, (93) becomes

$$\begin{aligned}\dot{s}_6 &= l_6\left(g_6\left(z_7 + e_7 + x_{7d}\right) - \dot{\sigma}_{61} + \varphi_6 z_6\left(0\right)\exp\left(-\varphi_6 t\right)\right)\\ &= l_6(g_6 z_7 + g_6 e_7 - a_6\mathrm{sig}(s_6)^{\alpha_6} - b_6 F_6(s_6) - c_6 s_6\\ &\quad - g_5 s_5 + \sigma_{62} - \dot{\sigma}_{61})\end{aligned} \tag{96}$$

Step 2.3 (Actual Control Input for the Throttle Setting): The sliding surface s_7 and its time derivative $\dot{s}_7$ are expressed as follows

$$s_7 = l_7\left(z_7 - z_7\left(0\right)\exp\left(-\varphi_7 t\right)\right) \tag{97}$$

$$\dot{s}_7 = l_7(g_7 u_2 + f_7 + d_7 - \dot{\sigma}_{71} + \varphi_7 z_7\left(0\right)\exp\left(-\varphi_7 t\right)) \tag{98}$$

where $l_7 \geq 1$, $\varphi_7 > 0$, $z_7(0)$ is the initial error of x_7.

Finally, the actual control input u_2 is designed as

$$\begin{aligned}u_2 = -\frac{1}{g_7}(&f_7 + \hat{d}_7 - \sigma_{72} + \varphi_7 z_7\left(0\right)\exp\left(-\varphi_7 t\right)\\ &+ a_7\mathrm{sig}(s_7)^{\alpha_7} + b_7 F_7(s_7) + c_7 s_7 + g_6 s_6)\end{aligned} \tag{99}$$

where a_7, b_7 and c_7 are positive constants, $\alpha_7 > 1$, $0 < \beta_7 < 1$, d_7 is estimated by SSTDOB. $F_7(s_7)$ is constructed as

$$F_7(s_7) = \begin{cases}\mathrm{sig}(s_7)^{\beta_7}, & |s_7| \geq \varepsilon_7\\ \tau_{71}s_7 + \tau_{72}s_7^2\mathrm{sign}\left(s_7\right), & |s_7| < \varepsilon_7\end{cases} \tag{100}$$

where $0 < \beta_7 < 1$, ε_7 is a small enough positive constant, $\tau_{71} = (2-\beta_7)\,\varepsilon_7^{\beta_7-1}$, $\tau_{72} = (1-\beta_7)\,\varepsilon_7^{\beta_7-2}$.

Substituting (99) into (98), we have

$$\dot{s}_7 = l_7(\tilde{d}_7 - a_7\mathrm{sig}(s_7)^{\alpha_7} - b_7 F_7(s_7) - c_7 s_7 - g_6 s_6 + \sigma_{72} - \dot{\sigma}_{71}) \tag{101}$$

where $\tilde{d}_7 = d_7 - \hat{d}_7$.

C. STABILITY ANALYZATION FOR SSTDOB-FSMC

In this section, the stability of the closed-loop system is analyzed by the Lyapunov theory.

Theorem 2: Consider the AHV system (16) and (17) with designed control inputs (66), (72), (78), (83), (88), (94), (99), and FTD (68), (74), (79), (90), (95) as well as SSTDOB (21). The closed-loop system is able to guarantee sliding surfaces and tracking errors converge to a small neighborhood of origin.

Proof: The Lyapunov function can be constructed as

$$L = \sum_{i=1}^{7}\frac{1}{2l_i}s_i^2 \tag{102}$$

Taking the time derivative of L yields

$$\dot{L} = \sum_{i=1}^{7}\frac{1}{l_i}s_i\dot{s}_i \tag{103}$$

Substituting (69), (75), (80), (85), (91), (96) and (101) into (103), we obtain

$$\begin{aligned}\dot{L} = &-\sum_{i=1}^{7}a_i|s_i|^{\alpha_i+1} - \sum_{i=1}^{7}b_i s_i F_i(s_i) - \sum_{i=1}^{7}c_i s_i^2\\ &+ \sum_{i=2,4,5,7}s_i\tilde{d}_i + \sum_{i=1,i\neq4}^{6}g_i s_i(z_{i+1} - s_{i+1})\\ &+ \sum_{i=1,i\neq4}^{6}g_i s_i e_{i+1} + \sum_{i=1,i\neq4}^{6}s_i(\sigma_{i+1,2} - \dot{\sigma}_{i+1,1})\end{aligned} \tag{104}$$

Since ε_i is small enough, the switching effect caused by $F_i(s_i)$ can be omitted. Thus, (104) can be reformed as

$$\begin{aligned}\dot{L} &= -\sum_{i=1}^{7}a_i|s_i|^{\alpha_i+1} - \sum_{i=1}^{7}b_i|s_i|^{\beta_i+1} - \sum_{i=1}^{7}c_i s_i^2\\ &\quad + \sum_{i=2,4,5,7}s_i\tilde{d}_i + \sum_{i=1,i\neq4}^{6}g_i s_i(z_{i+1} - s_{i+1})\\ &\quad + \sum_{i=1,i\neq4}^{6}g_i s_i e_{i+1} + \sum_{i=1,i\neq4}^{6}s_i(\sigma_{i+1,2} - \dot{\sigma}_{i+1,1})\\ &= -\sum_{i=1}^{7}a_i|s_i|^{\alpha_i+1} - \sum_{i=1}^{7}b_i|s_i|^{\beta_i+1} - \sum_{i=1}^{7}c_i s_i^2\\ &\quad + \sum_{i=1,i\neq4}^{6}g_i s_i((\frac{1}{l_{i+1}} - 1)s_{i+1} + z_{i+1}(0)\exp(-\varphi_{i+1}t))\\ &\quad + \sum_{i=1,i\neq4}^{6}g_i s_i e_{i+1} + \sum_{i=2,4,5,7}s_i\tilde{d}_i\\ &\quad + \sum_{i=1,i\neq4}^{6}s_i(\sigma_{i+1,2} - \dot{\sigma}_{i+1,1})\end{aligned} \tag{105}$$

Based on the left half side of inequalities in (63), one can get

$$\begin{aligned}\dot{L} \leq &-\sum_{i=1}^{7}a_i s_i^2 - \sum_{i=1}^{7}b_i|s_i|^{\alpha_i+1} - \sum_{i=1}^{7}c_i|s_i|^{\beta_i+1}\\ &+ \sum_{i=1,i\neq4}^{6}g_i s_i(\frac{1}{l_{i+1}} - 1)s_{i+1}\\ &+ \sum_{i=1,i\neq4}^{6}g_i s_i|z_{i+1}(0)|\exp(-\varphi_{i+1}t)\\ &+ \sum_{i=1,i\neq4}^{6}g_i s_i e_{i+1} + \sum_{i=2,4,5,7}s_i\tilde{d}_i\\ &+ \sum_{i=1,i\neq4}^{6}s_i(\sigma_{i+1,2} - \dot{\sigma}_{i+1,1})\end{aligned} \tag{106}$$

Since $\varphi_i > 0$, we have $|\exp(-\varphi_i t)| \leq 1$, and (106) becomes

$$\begin{aligned}\dot{L} \leq & -\sum_{i=1}^{7} a_i s_i^2 - \sum_{i=1}^{7} b_i |s_i|^{\alpha_i+1} - \sum_{i=1}^{7} c_i |s_i|^{\beta_i+1} \\ & + \sum_{i=1,i\neq 4}^{6} g_i s_i (\frac{1}{l_{i+1}} - 1) s_{i+1} + \sum_{i=1,i\neq 4}^{6} g_i s_i |z_{i+1}(0)| \\ & + \sum_{i=1,i\neq 4}^{6} g_i s_i e_{i+1} + \sum_{i=2,4,5,7} s_i \tilde{d}_i \\ & + \sum_{i=1,i\neq 4}^{6} s_i (\sigma_{i+1,2} - \dot{\sigma}_{i+1,1}) \end{aligned} \tag{107}$$

According to (42), if $t > \max(t_i)$, $i = 2, 4, 5, 7$, $\tilde{d}_i = 0$ are all satisfied. With Lemma 3 and its conclusion in Remark 6,we have $e_j = 0$, $j = 2, 3, 4, 6, 7$, and $\dot{\sigma}_{j+1,1} = \sigma_{j+1,2}$ when $t > \max(t_i) + \max(t_{FTDj})$. Thus, (107) becomes

$$\begin{aligned}\dot{L} \leq & -\sum_{i=1}^{7} a_i |s_i|^{\alpha_i+1} - \sum_{i=1}^{7} b_i |s_i|^{\beta_i+1} - \sum_{i=1}^{7} c_i s_i^2 \\ & + \sum_{i=1,i\neq 4}^{6} |g_i| (\frac{1}{l_{i+1}} - 1) |s_i| |s_{i+1}| \\ & + \sum_{i=1,i\neq 4}^{6} |g_i| |s_i| \eta_{i+1} \end{aligned} \tag{108}$$

Using Young's inequality and Assumption 3, we yield

$$\begin{aligned}\dot{L} \leq & -\sum_{i=1}^{7} a_i \left(s_i^2\right)^{\frac{\alpha_i+1}{2}} - \sum_{i=1}^{7} b_i \left(s_i^2\right)^{\frac{\beta_i+1}{2}} - \sum_{i=1}^{7} c_i s_i^2 \\ & + \sum_{i=1,i\neq 4}^{6} \bar{g}_i (\frac{1}{l_{i+1}} - 1) \frac{s_i^2 + s_{i+1}^2}{2} + \sum_{i=1,i\neq 4}^{6} \bar{g}_i \frac{s_i^2 + \eta_{i+1}^2}{2} \\ \leq & -\sum_{i=1}^{7} a_i \left(s_i^2\right)^{\frac{\alpha_i+1}{2}} - \sum_{i=1}^{7} b_i \left(s_i^2\right)^{\frac{\beta_i+1}{2}} - \sum_{i=1}^{7} c_i s_i^2 \\ & + \sum_{i=1,i\neq 4}^{6} \bar{g}_i (\frac{1}{l_{i+1}} - 1) \left(s_i^2 + s_{i+1}^2\right) \\ & + \sum_{i=1,i\neq 4}^{6} \bar{g}_i s_i^2 + \sum_{i=1,i\neq 4}^{6} \bar{g}_i \eta_{i+1}^2 \end{aligned} \tag{109}$$

Merging all the same items of (109), we obtain

$$\begin{aligned}\dot{L} \leq & -\sum_{i=1}^{7} a_i l_i^{\frac{\alpha_i+1}{2}} (\frac{s_i^2}{l_i})^{\frac{\alpha_i+1}{2}} - \sum_{i=1}^{7} b_i l_i^{\frac{\beta_i+1}{2}} (\frac{s_i^2}{l_i})^{\frac{\beta_i+1}{2}} \\ & + (\frac{\bar{g}_1}{l_2} - c_1) l_1 \frac{s_1^2}{l_1} + (\frac{\bar{g}_2}{l_3} + \frac{\bar{g}_1}{l_2} - \bar{g}_1 - c_2) l_2 \frac{s_2^2}{l_2} \\ & + (\frac{\bar{g}_3}{l_4} + \frac{\bar{g}_2}{l_3} - \bar{g}_2 - c_3) l_3 \frac{s_3^2}{l_3} \\ & + (\frac{\bar{g}_3}{l_4} - \bar{g}_3 - c_4) l_4 \frac{s_4^2}{l_4} + (\frac{\bar{g}_5}{l_6} - c_5) l_5 \frac{s_5^2}{l_5} \\ & + (\frac{\bar{g}_6}{l_7} + \frac{\bar{g}_5}{l_6} - \bar{g}_5 - c_6) l_6 \frac{s_6^2}{l_6} \\ & + (\frac{\bar{g}_6}{l_7} - \bar{g}_6 - c_7) l_7 \frac{s_7^2}{l_7} + \sum_{i=1,i\neq 4}^{6} \bar{g}_i \eta_{i+1}^2 \end{aligned} \tag{110}$$

Setting $A = \min(a_i l_i^{\frac{\alpha_i+1}{2}})(i = 1, 2, \cdots, 7)$, $B = \min(b_i l_i^{\frac{\beta_i+1}{2}})$, $K = \max((\frac{\bar{g}_1}{l_2} - c_1) l_1, (\frac{\bar{g}_2}{l_3} + \frac{\bar{g}_1}{l_2} - \bar{g}_1 - c_2) l_2, (\frac{\bar{g}_3}{l_4} + \frac{\bar{g}_2}{l_3} - \bar{g}_2 - c_3) l_3, (\frac{\bar{g}_3}{l_4} - \bar{g}_3 - c_4) l_4, (\frac{\bar{g}_5}{l_6} - c_5) l_5, (\frac{\bar{g}_6}{l_7} + \frac{\bar{g}_5}{l_6} - \bar{g}_5 - c_6) l_6, (\frac{\bar{g}_6}{l_7} - \bar{g}_6 - c_7) l_7)$ and $\Gamma_0 = \sum_{i=1,i\neq 4}^{6} \bar{g}_i \eta_{i+1}^2$, (110) becomes

$$\dot{L} \leq -A \sum_{i=1}^{7} (\frac{s_i^2}{l_i})^{\frac{\alpha_i+1}{2}} - B \sum_{i=1}^{7} (\frac{s_i^2}{l_i})^{\frac{\beta_i+1}{2}} + K \sum_{i=1}^{7} \frac{s_i^2}{l_i} + \Gamma_0 \tag{111}$$

By applying the inequality $x \leq x^p + x^q$ [38], where $x > 0, p > 1, 0 < q < 1$, one gets

$$\begin{aligned}\dot{L} \leq & -A \sum_{i=1}^{7} (\frac{s_i^2}{l_i})^{\frac{\alpha_i+1}{2}} - B \sum_{i=1}^{7} (\frac{s_i^2}{l_i})^{\frac{\beta_i+1}{2}} + K \sum_{i=1}^{7} (\frac{s_i^2}{l_i})^{\frac{\alpha_i+1}{2}} \\ & + K \sum_{i=1}^{7} (\frac{s_i^2}{l_i})^{\frac{\beta_i+1}{2}} + \Gamma_0 \\ = & -(A - K) \sum_{i=1}^{7} (\frac{s_i^2}{l_i})^{\frac{\alpha_i+1}{2}} - (B - K) \sum_{i=1}^{7} (\frac{s_i^2}{l_i})^{\frac{\beta_i+1}{2}} + \Gamma_0 \end{aligned} \tag{112}$$

Setting $\alpha_i = r_1$, $\beta_i = r_2$ $(i = 1, 2, \ldots, 7)$, we have

$$\begin{aligned}\dot{L} \leq & -(A - K)(\sum_{i=1}^{7} (\frac{s_i^2}{l_i}))^{\frac{r_1+1}{2}} - (B - K)(\sum_{i=1}^{7} (\frac{s_i^2}{l_i}))^{\frac{r_2+1}{2}} \\ & + \Gamma_0 \\ \leq & -\Gamma_1 L^{\frac{r_1+1}{2}} - \Gamma_2 L^{\frac{r_2+1}{2}} + \Gamma_0 \end{aligned} \tag{113}$$

where $\Gamma_1 = 2^{\frac{r_1+1}{2}} \min(A, K)$, $\Gamma_2 = 2^{\frac{r_2+1}{2}} \min(B, K)$.

It is apparent that A, B and Γ_0 are positive, $K > 0$ is satisfied by choosing appropriate parameters. Then we obtain $\Gamma_1 > 0, \Gamma_2 > 0, \frac{r_1+1}{2} > 1, 0 < \frac{r_2+1}{2} < 1$. According to Lemma 1, the sliding surface will get close to a small region of zero in fixed time.

The convergence region 2Ω and the convergence time T_1 are calculated by

$$\Gamma_0 = \Gamma_1 \Omega^{\frac{r_1+1}{2}} + \Gamma_2 \Omega^{\frac{r_2+1}{2}} \tag{114}$$

$$T_1 < \frac{1}{\Gamma_1} \frac{2}{r_1 - 1} + \frac{1}{\Gamma_2 (2^{\frac{r_2+1}{2}})} \frac{2}{1 - r_2} \tag{115}$$

Therefore, the whole convergence time T evaluated by (42), (59) and (115) is derived as

$$\begin{aligned} T < & \max(t_i) + \max(t_{FTDj}) + T_1 \\ & (i = 2, 4, 5, 7; j = 2, 3, 4, 6, 7) \end{aligned} \tag{116}$$

Besides, according to (114), the sliding surfaces s_i $(i = 1, 2, \ldots, 7)$ will satisfy

$$|s_i| = |l_i(z_i - z_i(0)\exp(-\varphi_i t))| \leq 2\Omega \quad (i = 1, 2, \ldots, 7) \tag{117}$$

Calculating the limit of following equation yields

$$\lim_{t\to\infty} z_i(0)\exp(-\varphi_i t) = 0 \quad (i = 1, 2, \ldots, 7) \tag{118}$$

Then by substituting (118) into (117), the convergence region of tracking errors z_i can be transformed into

$$|z_i| \leq \frac{2\Omega}{l_i} \leq \bar{\Omega} \quad (i = 1, 2, \ldots, 7) \tag{119}$$

where $\bar{\Omega} = \frac{2\Omega}{\min(l_i, i=1,2,\ldots,7)}$.

The proof of Theorem 2 is completed.

Remark 8: In the fore designing process, we combine BC strategy with tracking differentiator, sliding mode control, fixed-time control, as well as disturbance observer, in an attempt to make the composite controller more robust and effective. The explosion problem is solved by utilizing a fixed-time tracking differentiator and the disturbance observer is employed at each corresponding step to compensate the lumped disturbances. Compared with conventional sliding mode backstepping control, the sliding surfaces selected in each design steps can improve the convergence speed and modify the state trajectories right from the beginning by adding an exponential term. Besides, the convergence time of proposed FSMBC is independent of initial condition and the singularity problem in the derivative of virtual control is improved by introducing a switching logic.

Remark 9: From the viewpoint of practical application, the energy of each system is limited. Therefore, it is reasonable to claim the boundedness mentioned in Assumption 3-5.

V. SIMULATION RESULTS

In this section, several simulations are conducted to demonstrate the performance of proposed control scheme. The initial simulation conditions and model parameters are given in Table 1 and Table 2. Besides, Earth related constants are $\mu = 3.98842 \times 10^{14}\text{N} \cdot \text{m}^2/\text{kg}$ and $R_E = 6.371 \times 10^6\text{m}$. The density of air can be defined as $\rho = \rho_0 \exp(-h/H_s)$ with $\rho_0 = 1.225\text{kg}/\text{m}^3$ is the density of air at sea level, $H_s = 7200\text{m}$ is the scale height.

TABLE 1. Initial state of AHV sytstem.

State	Value	State	Value	State	Value
V(m/s)	4000	h(m)	33000	$\theta(^\circ)$	0
$\vartheta(^\circ)$	2.7203	$\omega_z(^\circ)$	0	$\delta_e(^\circ)$	-0.5460
$\dot{\beta}$	0	β	0.2111	β_c	0.2111

As a representative case study, the desired altitude command h_d and desired velocity command V_d are generated by the following low-pass filters with their initial values at $h_d(0) = 33000$, $\dot{h}_d(0) = 0$, $V_d(0) = 4000$, $\dot{V}_d(0) = 0$

$$h_d(s) = \frac{87.5}{(s + 0.05)^2}, V_d(s) = \frac{40.5}{(s + 0.1)^2}$$

TABLE 2. Model parameters of AHV system.

Parameters	Value
m(kg)	1.368×10^5
$J_z(\text{kg} \cdot \text{m}^2)$	9.491×10^6
$S(\text{m}^2)$	334
l(m)	24.384
c_L^α	0.6203
c_D^0	3.772×10^{-3}
c_D^α	4.3378×10^{-3}
$c_D^{\alpha^2}$	0.645
c_T^0	$\begin{cases} 0, \beta < 1 \\ 0.0224, \beta \geq 1 \end{cases}$
c_T^β	$\begin{cases} 0.02576, \beta < 1 \\ 3.36 \times 10^{-3}, \beta \geq 1 \end{cases}$
m_z^0	5.3261×10^{-6}
m_z^α	7.417×10^{-3}
$m_z^{\alpha^2}$	-0.035
$m_z^{\omega_z}$	$\frac{l}{2V}\left(-6.796\alpha^2 + 0.3015\alpha - 0.2289\right)$
$m_z^{\delta_e}$	0.0292

In addition, constraints of the actuators and the external disturbances are listed as

$$\begin{cases} |\delta_e| \leq 30^\circ \\ 0 \leq \beta_c \leq 1 \end{cases}$$

$$d_2(t) = \begin{cases} 0 & 0 \leq t < 100 \\ 0.01\sin(0.1\pi t) & 100 \leq t < 325 \\ 0.01 & 325 \leq t < 400 \end{cases}$$

$$d_4(t) = \begin{cases} 0 & 0 \leq t < 80 \\ 0.005t - 0.4 & 80 \leq t < 100 \\ 0.1 & 100 \leq t < 250 \\ 0.1\sin(0.1\pi t) & 250 \leq t < 400 \end{cases}$$

$$d_5(t) = \begin{cases} 0 & 0 \leq t < 150 \\ 0.5\sin(0.02\pi t) & 150 \leq t < 400 \end{cases}$$

$$d_7(t) = \begin{cases} 0 & 0 \leq t < 100 \\ 0.001t - 0.1 & 100 \leq t < 200 \\ 0.1 + 0.1\sin(0.1\pi t) & 200 \leq t < 400 \end{cases}$$

To verify the performance of the proposed controller (SSTDOB-FSMBC), the simulation results are divided into two groups as follows:

Group 1: Simulation on the AHV longitudinal model without aerodynamic uncertainties.

In this group, comparisons among SSTDOB-FSMBC, conventional super twisting disturbance observer based sliding mode control (CSTDOB-SMC) mentioned in Wang *et al.* [29] and a strictly-lower-convex-function based nonlinear disturbance observer based adaptive terminal sliding mode control (SDOB-ATSMC) designed in Wu *et al.* [26] are given to illustrate the robustness of proposed control approach.

Besides, the parameters of each control scheme are listed as follows.

SSTDOB-FSMBC:

$$
\begin{aligned}
&p_2 = p_4 = p_5 = p_7 = 2,\\
&k_{21} = 2,\ k_{22} = 3,\ k_{23} = 1.5,\ k_{24} = 6,\\
&k_{41} = 1.5,\ k_{42} = 3,\ k_{43} = 1,\ k_{44} = 6,\\
&k_{51} = 2,\ k_{52} = 4,\ k_{53} = 1,\ k_{54} = 7,\\
&k_{71} = 2,\ k_{72} = 3,\ k_{73} = 1.7,\ k_{74} = 7,\\
&\lambda_{j1} = 4,\ \lambda_{j2} = 10,\ \kappa_{j1} = 4,\ \kappa_{j2} = 10,\ j = 2, 3, 4, 6, 7,\\
&l_i = 1,\ \varphi_i = 10,\ \alpha_i = r_1 = 1.2,\ \beta_i = r_2 = 0.8,\ i = 1, \cdots, 7,\\
&a_1 = 1.1,\ a_2 = 2,\ a_3 = 2,\ a_4 = 1,\ a_5 = 2,\ a_6 = 2,\ a_7 = 1,\\
&b_1 = 0.01,\ b_2 = 0.3,\ b_3 = 0.5,\ b_4 = 0.5,\ b_5 = b_6 = b_7 = 0.9,\\
&c_1 = c_2 = c_3 = c_4 = c_5 = c_6 = c_7 = 0.1.
\end{aligned}
$$

CSTDOB-SMC:

$$
\begin{aligned}
&\omega_{11} = 0.1, \omega_{21} = 0.01, \omega_{12} = 0.1, \omega_{22} = 0.02,\\
&k_1 = 0.2, k_2 = 0.3, \gamma_1 = 0.95, \gamma_2 = 0.95.
\end{aligned}
$$

SDOB-ATSMC:

$$
\begin{aligned}
&u = (\frac{5x_2^4}{6} + 5x_2^2) + (\frac{x_4^6}{3} + \frac{5x_4^4}{6} + 5x_4^2) + 5x_5^2 + (\frac{5x_7^4}{6} + 5x_7^2),\\
&\Lambda = 60I_3, c_1 = 1, c_5 = 2,\\
&\tau_1 = 1, \tau_2 = 0.7, \tau_3 = 1.7, \tau_4 = 0.65, \tau_5 = 12, \tau_6 = 6, \tau_7 = 1,\\
&r_1 = r_2 = r_3 = r_4 = \frac{7}{9}, r_5 = r_6 = r_7 = 0.95,\\
&\sigma_1 = 0.2, \sigma_2 = 0.3, \sigma_3 = 0.25, \sigma_4 = 0.4,\\
&\sigma_5 = 0.3, \sigma_6 = 0.4, \sigma_7 = 0.7.
\end{aligned}
$$

Group 2: Simulation on the AHV longitudinal model with aerodynamic uncertainties.

In this scenario, the simulations of proposed scheme considering external disturbances and aerodynamic uncertainties are performed. The control parameters of SSTDOB-FSMBC are same to that of Group 1. Here, the atmospheric force and moment coefficients can be rewritten as

$$
\begin{aligned}
C_T &= C_T^*(1 + \Delta_{fT})C_D = C_D^*(1 + \Delta_{fD})\\
C_L &= C_L^*(1 + \Delta_{fL})C_{mz} = C_L^*(1 + \Delta_{fM})
\end{aligned}
$$

where $C_\cdot^*$ and $\Delta_{f\cdot}$ are the nominal value and fixed parameter uncertainty, respectively.

A. SIMULATION ANALYSIS OF SSTDOB-FSMBC WITHOUT AERODYNAMIC UNCERTAINTIES

Figures 3 and 4 show the tracking curves of altitude h and velocity V, respectively. It can be observed that all these controllers show satisfactory performances when the disturbances are not involved in the first 100 seconds. In the presence of external disturbances, the proposed SSTDOB-FSMBC performs well in tracking of altitude and velocity command, whereas the CSDOB-SMC and SDOB-ATSMC exhibit worse because of their weaker disturbance rejection. Besides, Figures 3 and 4 also reveal that SSTDOB-FSMBC has faster convergence rate without overshoot, and other methods will produce slow convergence with undesired large overshoot, which suggests that the proposed

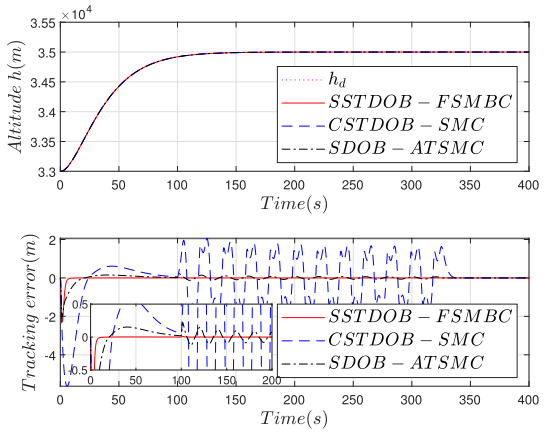

FIGURE 3. Tracking curves of altitude *h* for Group 1.

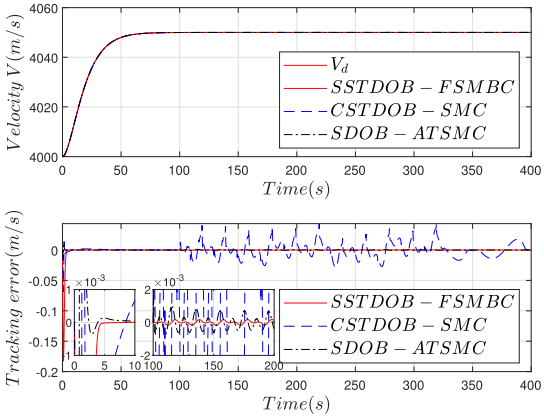

FIGURE 4. Tracking curves of velocity *V* for Group 1.

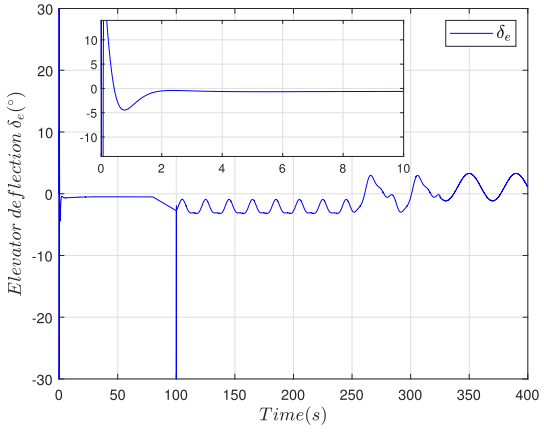

FIGURE 5. Elevator deflection angle δ_e for Group 1.

SSTDOB-FSMBC is more effective than CSDOB-SMC and SDOB-ATSMC.

Figures 5 and 6 represent the control inputs of elevator deflection angle δ_e and demand of throttle setting β_c, respectively. As shown in the simulation results, the control inputs δ_e and β_c vary in their constraints during the whole process.

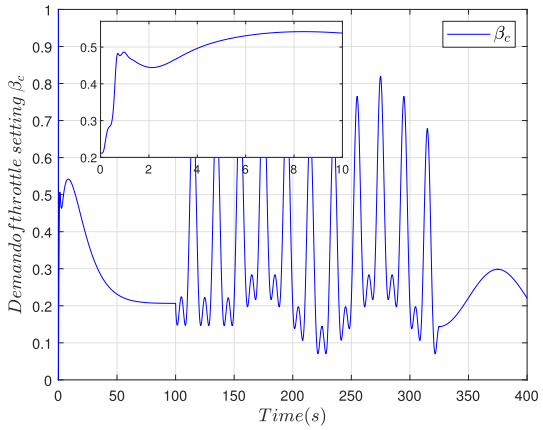

FIGURE 6. Demand of throttle setting β_c for Group 1.

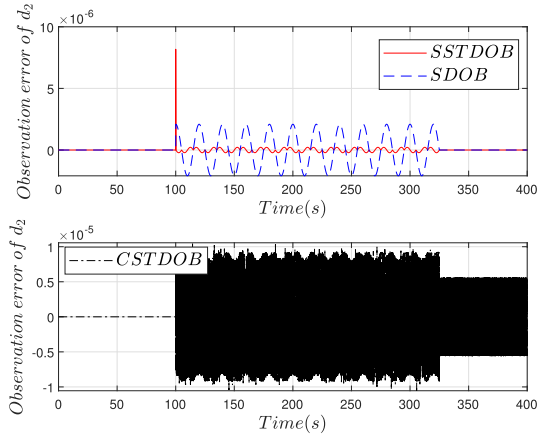

FIGURE 7. Observation error of d_2.

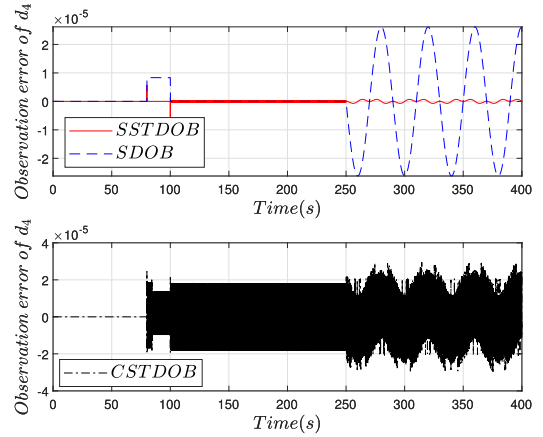

FIGURE 8. Observation error of d_4.

The estimation results of proposed SSTDOB are depicted in Figures 7-10. Since the sign function will directly appear in the CSTDOB, serious chattering may exist when the observation errors vary in the neighbor of zero, which would cause a variety of troubles in practical systems. As for the SSTDOB, the possible sign function can be hidden in the integral items, then the outputs of SSTDOB will become continuous and the chattering phenomenon is well eliminated.

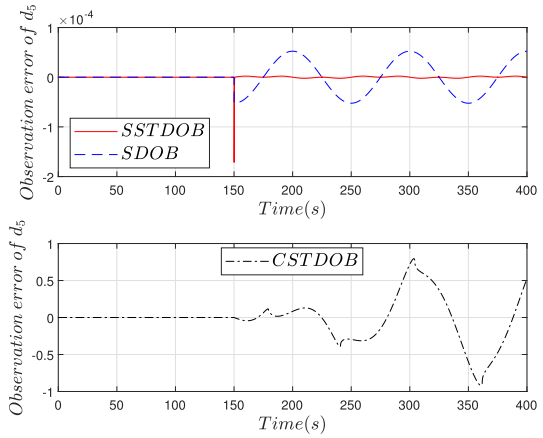

FIGURE 9. Observation error of d_5.

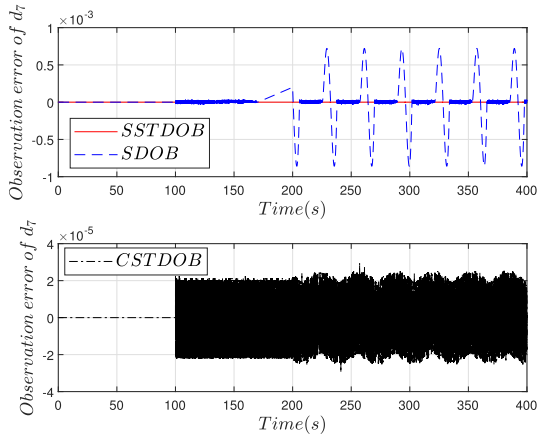

FIGURE 10. Observation error of d_7.

Therefore, the curves of SSTDOB are much smoother than that of CSTDOB. The outputs of SDOB are also smoother than CSTDOB because of the low-convex-function designed in SDOB. Howbeit, we can see that the estimation errors of SDOB are larger than that of SSTDOB. Besides, it is shown in Figure 10 that CSTDOB exhibits poor observation performance for disturbances with faster change rates. This result will further explain the vibrations of CSTDOB-SMC's tracking curves in Figures 3 and 4. The above analysis also indicates that SSTDOB do has a better disturbance observation ability than CSTDOB and SDOB. Thus, this SSTDOB can enhance the robustness of proposed controller.

Figures 11 and 12 demonstrate the time response of sliding surfaces $s_1, s_2, \ldots, s_7$. It is observed that the sliding surfaces of s_1, s_2, s_3 and s_4 converge to the region of zero in about 20s, s_5, s_6, and s_7 converge to the region of zero in about 10s.

B. SIMULATION ANALYSIS OF SSTDOB-FSMBC WITH AERODYNAMIC UNCERTAINTIES

In order to examine the control performance of proposed SSTDOB-FSMBC under aerodynamic uncertainties, we select the uncertainties as follows.

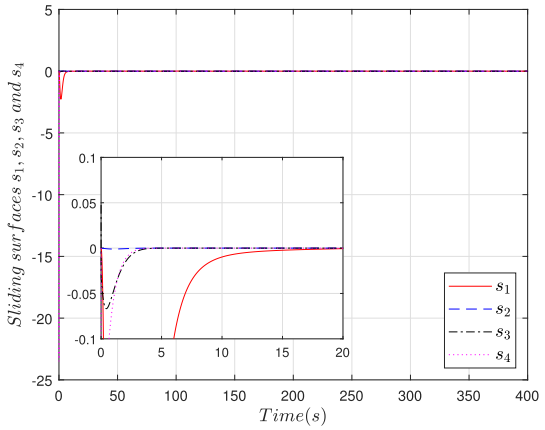

FIGURE 11. Sliding surfaces of s_1, s_2, s_3 and s_4.

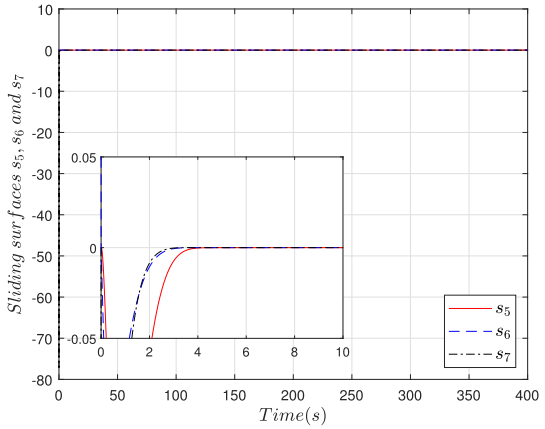

FIGURE 12. Sliding surfaces of s_5, s_6 and s_7.

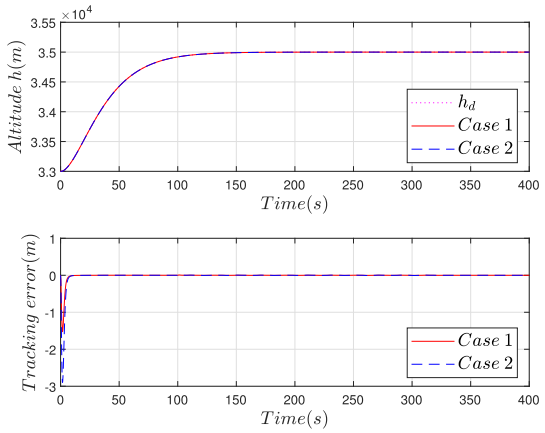

FIGURE 13. Tracking curves of altitude *h* for Group 2.

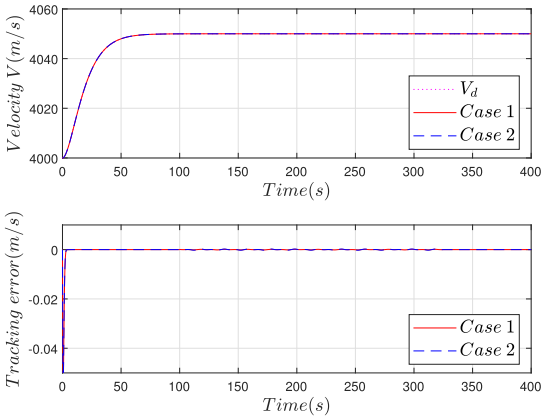

FIGURE 14. Tracking curves of velocity *V* for Group 2.

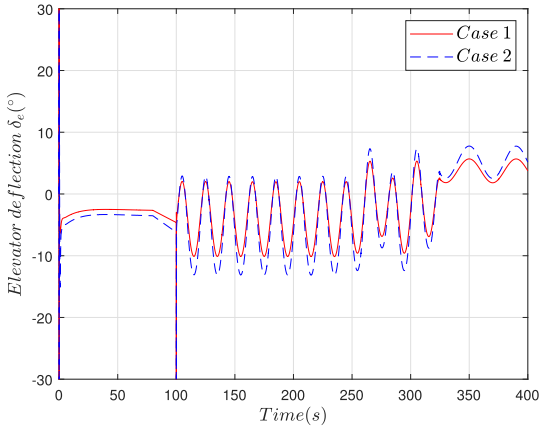

FIGURE 15. Elevator deflection angle δ_e for Group 2.

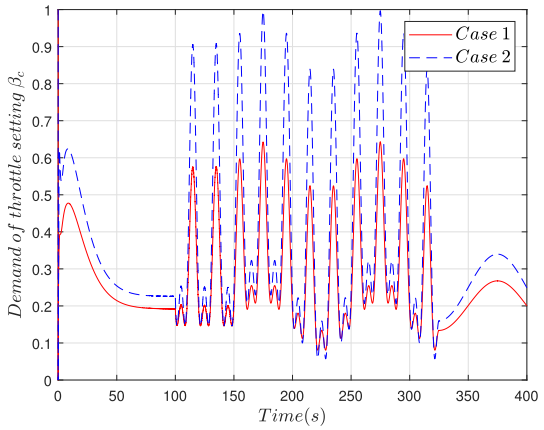

FIGURE 16. Demand of throttle setting δ_e for Group 2.

Case 1: $\Delta_{fT} = 20\%$, $\Delta_{fD} = 20\%$, $\Delta_{fL} = 20\%$, $\Delta_{fM} = 20\%$

Case 2: $\Delta_{fT} = -20\%$, $\Delta_{fD} = -20\%$, $\Delta_{fL} = -20\%$, $\Delta_{fM} = -20\%$.

The tracking curves of altitude h and velocity V are shown in Figures 13 and 14. The simulation results demonstrate that proposed control scheme can still present rapid convergence rate and excellent tracking precision in the presence of external disturbances and parameter uncertainties.

Figure 15 displays the curves of control inputs elevator deflection angle δ_e. Figure 16 shows the demand of throttle setting β_c. It can be seen that when Case 1 and Case 2 are introduced respectively, the control inputs δ_e and β_c still satisfy the constraints. Therefore, we can draw a conclusion

that the proposed controller possesses fast convergence rate and excellent anti-interference ability.

VI. CONCLUSION AND FUTURE WORK

In this paper, a robust composite control scheme SSTDOB-FSMBC is developed to achieve the attitude and velocity tracking of AHV. The SSTDOB is firstly designed to estimate the disturbances exhibited in AHV, which can effectively enhance the anti-interference performance of control system. Moreover, the ''explosion of complexity'' inherent in conventional BC is avoided by utilizing a fixed-time tracking differentiator. In order to improve the singularity problem caused by the derivative of virtual control in FSMBC, we introduce a switching logic. Then, the stability of closed-loop system is proven by Lyapunov method. Simulation results illustrate the effectiveness of proposed SSTDOB-FSMBC. In this paper, we just consider the amplitude limit of control inputs, which is relatively simple. Future work will focus on the AHV's fixed-time control problem with input saturations and full state constraints.

REFERENCES

[1] B. Xu and Z. Shi, ''An overview on flight dynamics and control approaches for hypersonic vehicles,'' *Sci. China Inf. Sci.*, vol. 58, no. 7, pp. 1–19, Jul. 2015.
[2] F. Wang, Q. Zou, Q. Zong, and C. Hua, ''Adaptive prescribed performance fault tolerant control for a flexible air-breathing hypersonic vehicle with uncertainty,'' *IEEE Access*, vol. 7, pp. 35018–35033, 2019.
[3] J. Zheng, J. Chang, J. Ma, and D. Yu, ''Modeling and analysis for integrated airframe/propulsion control of vehicles during mode transition of over-under turbine-based-combined-cycle engines,'' *Aerosp. Sci. Technol.*, vol. 95, Dec. 2019, Art. no. 105462.
[4] D. Zhang, S. Tang, Q.-J. Zhu, and R.-G. Wang, ''Analysis of dynamic characteristics of the rigid body/elastic body coupling of air-breathing hypersonic vehicles,'' *Aerosp. Sci. Technol.*, vol. 48, pp. 328–341, Jan. 2016.
[5] G. Wu, X. Meng, and F. Wang, ''Improved nonlinear dynamic inversion control for a flexible air-breathing hypersonic vehicle,'' *Aerosp. Sci. Technol.*, vol. 78, pp. 734–743, Jul. 2018.
[6] J. T. Parker, A. Serrani, S. Yurkovich, M. A. Bolender, and D. B. Doman, ''Control-oriented modeling of an air-breathing hypersonic vehicle,'' *J. Guid., Control, Dyn.*, vol. 30, no. 3, pp. 856–869, May 2007.
[7] D. O. Sigthorsson, P. Jankovsky, A. Serrani, S. Yurkovich, M. A. Bolender, and D. B. Doman, ''Robust linear output feedback control of an airbreathing hypersonic vehicle,'' *J. Guid., Control, Dyn.*, vol. 31, no. 4, pp. 1052–1066, Jul. 2008.
[8] T. E. Gibson, L. G. Crespo, and A. M. Annaswamy, ''Adaptive control of hypersonic vehicles in the presence of modeling uncertainties,'' in *Proc. Amer. Control Conf.*, St. Louis, MO, USA, Jun. 2009, pp. 3178–3183.
[9] L. Cao, S. Tang, and D. Zhang, ''Fractional-order sliding mode control of air-breathing hypersonic vehicles based on linear-quadratic regulator,'' *J. Aerosp. Eng.*, vol. 31, no. 3, May 2018, Art. no. 04018022.
[10] H. Li, J. Yu, C. Hilton, and H. Liu, ''Adaptive sliding-mode control for nonlinear active suspension vehicle systems using T–S fuzzy approach,'' *IEEE Trans. Ind. Electron.*, vol. 60, no. 8, pp. 3328–3338, Aug. 2013.
[11] X. Hu, B. Xu, and C. Hu, ''Robust adaptive fuzzy control for HFV with parameter uncertainty and unmodeled dynamics,'' *IEEE Trans. Ind. Electron.*, vol. 65, no. 11, pp. 8851–8860, Nov. 2018.
[12] X. Li and G. Li, ''Novel fuzzy approximation control scheme for flexible air-breathing hypersonic vehicles with non-affine dynamics and amplitude and rate constraints,'' *IEEE Access*, vol. 7, pp. 73602–73616, 2019.
[13] H. N. Wu, S. Feng, Z. Y. Liu, and L. Guo, ''Disturbance observer based robust mixed H_2/H_∞ fuzzy tracking control for hypersonic vehicles,'' *Fuzzy Sets Syst.*, vol. 306, pp. 118–136, Feb. 2016.
[14] X. W. Bu and Y. Xiao, ''Prescribed performance-based low-computational cost fuzzy control of a hypersonic vehicle using non-affine models,'' *Adv. Mech. Eng.*, vol. 10, no. 2, Feb. 2018, Art. no. 1687814018757261, doi: 10.1177/1687814018757261.
[15] B. Xu, D. Wang, F. Sun, and Z. Shi, ''Direct neural discrete control of hypersonic flight vehicle,'' *Nonlinear Dyn.*, vol. 70, no. 1, pp. 269–278, Oct. 2012.
[16] X. Bu, X. Wu, Z. Ma, and R. Zhang, ''Novel adaptive neural control of flexible air-breathing hypersonic vehicles based on sliding mode differentiator,'' *Chin. J. Aeronaut.*, vol. 28, no. 4, pp. 1209–1216, Aug. 2015.
[17] B. Xu, Z. Shi, C. Yang, and S. Wang, ''Neural control of hypersonic flight vehicle model via time-scale decomposition with throttle setting constraint,'' *Nonlinear Dyn.*, vol. 73, no. 3, pp. 1849–1861, Aug. 2013.
[18] X. Bu, X. Wu, M. Tian, J. Huang, R. Zhang, and Z. Ma, ''High-order tracking differentiator based adaptive neural control of a flexible air-breathing hypersonic vehicle subject to actuators constraints,'' *ISA Trans.*, vol. 58, pp. 237–247, Sep. 2015.
[19] Y. Ma and Y. Cai, ''A fuzzy model predictive control based upon adaptive neural network disturbance observer for a constrained hypersonic vehicle,'' *IEEE Access*, vol. 6, pp. 5927–5938, 2018.
[20] B. Xu, C. Yang, and Y. Pan, ''Global neural dynamic surface tracking control of strict-feedback systems with application to hypersonic flight vehicle,'' *IEEE Trans. Neural Netw. Learn. Syst.*, vol. 26, no. 10, pp. 2563–2575, Oct. 2015.
[21] X. Bu, G. He, and K. Wang, ''Tracking control of air-breathing hypersonic vehicles with non-affine dynamics via improved neural back-stepping design,'' *ISA Trans.*, vol. 75, pp. 88–100, Apr. 2018.
[22] S. Ding, K. Mei, and S. Li, ''A new second-order sliding mode and its application to nonlinear constrained systems,'' *IEEE Trans. Autom. Control*, vol. 64, no. 6, pp. 2545–2552, Jun. 2019.
[23] H. Xu, M. D. Mirmirani, and P. A. Ioannou, ''Adaptive sliding mode control design for a hypersonic flight vehicle,'' *J. Guid., Control, Dyn.*, vol. 27, no. 5, pp. 829–838, Sep. 2004.
[24] Q. Zong, J. Wang, B. Tian, and Y. Tao, ''Quasi-continuous high-order sliding mode controller and observer design for flexible hypersonic vehicle,'' *Aerosp. Sci. Technol.*, vol. 27, no. 1, pp. 127–137, Jun. 2013.
[25] Y. Yan and S. Yu, ''Sliding mode tracking control of autonomous underwater vehicles with the effect of quantization,'' *Ocean Eng.*, vol. 151, pp. 322–328, Mar. 2018.
[26] Y.-J. Wu, J.-X. Zuo, and L.-H. Sun, ''Adaptive terminal sliding mode control for hypersonic flight vehicles with strictly lower convex function based nonlinear disturbance observer,'' *ISA Trans.*, vol. 71, pp. 215–226, Nov. 2017.
[27] H. Sun, S. Li, and C. Sun, ''Finite time integral sliding mode control of hypersonic vehicles,'' *Nonlinear Dyn.*, vol. 73, nos. 1–2, pp. 229–244, Jul. 2013.
[28] X. Yang, J. Li, and Y. Dong, ''Flexible air-breathing hypersonic vehicle control based on a novel non-singular fast terminal sliding mode control and nonlinear disturbance observer,'' *Proc. Inst. Mech. Eng. G, J. Aerosp. Eng.*, vol. 231, no. 11, pp. 2132–2145, Sep. 2017.
[29] J. Wang, Y. Wu, and X. Dong, ''Recursive terminal sliding mode control for hypersonic flight vehicle with sliding mode disturbance observer,'' *Nonlinear Dyn.*, vol. 81, no. 3, pp. 1489–1510, Aug. 2015.
[30] Y. Yan, S. Yu, and X. Yu, ''Quantized super-twisting algorithm based sliding mode control,'' *Automatica*, vol. 105, pp. 43–48, Jul. 2019.
[31] A. Polyakov, ''Nonlinear feedback design for fixed-time stabilization of linear control systems,'' *IEEE Trans. Autom. Control.*, vol. 57, no. 8, pp. 2106–2110, Aug. 2012.
[32] X. Yu, P. Li, and Y. Zhang, ''The design of fixed-time observer and finite-time fault-tolerant control for hypersonic gliding vehicles,'' *IEEE Trans. Ind. Electron.*, vol. 65, no. 5, pp. 4135–4144, May 2018.
[33] B. L. Tian, H. C. Lu, Z. Y. Zuo, and W. Yang, ''Fixed-time leader–follower output feedback consensus for second-order multiagent systems,'' *IEEE Trans. Cybern.*, vol. 49, no. 4, pp. 1545–1550, Feb. 2018.
[34] G. Li, Y. Wu, and P. Xu, ''Adaptive fault-tolerant cooperative guidance law for simultaneous arrival,'' *Aerosp. Sci. Technol.*, vols. 82–83, pp. 243–251, Nov. 2018.
[35] Z. Zuo and L. Tie, ''A new class of finite-time nonlinear consensus protocols for multi-agent systems,'' *Int. J. Control*, vol. 87, no. 2, pp. 363–370, Feb. 2014.
[36] M. Basin, C. B. Panathula, and Y. Shtessel, ''Adaptive uniform finite-/fixed-time convergent second order sliding mode control,'' *Int. J. Control*, vol. 89, no. 9, p. 1777, 2016.
[37] X. Wang, J. Guo, S. Tang, and S. Qi, ''Fixed-time disturbance observer based fixed-time back-stepping control for an air-breathing hypersonic vehicle,'' *ISA Trans.*, vol. 88, pp. 233–245, May 2019.

[38] Y. Ding, X. Wang, Y. Bai, and N. Cui, "Robust fixed-time sliding mode controller for flexible air-breathing hypersonic vehicle," *ISA Trans.*, vol. 90, pp. 1–18, Jul. 2019.
[39] P. Li, J. Ma, and Z. Zheng, "Disturbance-observer-based fixed-time second-order sliding mode control of an air-breathing hypersonic vehicle with actuator faults," *Proc. Inst. Mech. Eng. G, J. Aerosp. Eng.*, vol. 232, no. 2, pp. 344–361, Feb. 2018.
[40] F. Wang, Y. Guo, K. Wang, Z. Zhang, C. Hua, and Q. Zong, "Disturbance observer based robust backstepping control design of flexible air-breathing hypersonic vehicle," *IET Control Theory Appl.*, vol. 13, no. 4, pp. 572–583, Mar. 2019.
[41] S. H. Ding, W. H. Chen, K. Q. Mei, and D. Murray-smith, "Disturbance observer design for nonlinear systems represented by input-output models," *IEEE Trans. Ind. Electron.*, vol. 67, no. 2, pp. 1222–1232, Feb. 2019.
[42] J. Tian, S. Zhang, Y. Zhang, and T. Li, "Active disturbance rejection control based robust output feedback autopilot design for airbreathing hypersonic vehicles," *ISA Trans.*, vol. 74, pp. 45–59, Mar. 2018.
[43] Y.-J. Wu and G.-F. Li, "Adaptive disturbance compensation finite control set optimal control for PMSM systems based on sliding mode extended state observer," *Mech. Syst. Signal Process.*, vol. 98, pp. 402–414, Jan. 2018.
[44] X. Bu, "Air-breathing hypersonic vehicles funnel control using neural approximation of non-affine dynamics," *IEEE/ASME Trans. Mechatronics*, vol. 23, no. 5, pp. 2099–2108, Oct. 2018.
[45] M. V. Basin, P. Yu, and Y. B. Shtessel, "Hypersonic missile adaptive sliding mode control using finite-and fixed-time observers," *IEEE Trans. Ind. Electron.*, vol. 65, no. 1, pp. 930–941, Jan. 2018.
[46] J. Yu, P. Shi, and L. Zhao, "Finite-time command filtered backstepping control for a class of nonlinear systems," *Automatica*, vol. 92, pp. 173–180, Jun. 2018.
[47] J. Li, Y. Yang, C. Hua, and X. Guan, "Fixed-time backstepping control design for high-order strict-feedback non-linear systems via terminal sliding mode," *IET Control Theory Appl.*, vol. 11, no. 8, pp. 1184–1193, May 2017.
[48] I. Nagesh and C. Edwards, "A multivariable super-twisting sliding mode approach," *Automatica*, vol. 50, no. 3, pp. 984–988, Mar. 2014.
[49] Z. G. Zhou, D. Zhou, X. N. Shi, R. F. Li, and B. Q. Kan, "Prescribed performance fixed-time tracking control for a class of second-order nonlinear systems with disturbances and actuator saturation," *Int. J. Control*, pp. 1–12, 2019, doi: 10.1080/00207179.2019.1590644.

YUNJIE WU was born in 1969. She received the Ph.D. degree in navigation guidance and control from Beihang University, Beijing, China, in 2006. She is currently a Professor with the School of Automation Science and Electrical Engineering, Beihang University. Her research interests include system simulation, intelligent control, servo control, aircraft guidance, and control technology.

FEI MA was born in 1993. He received the B.S. degree from the College of Automation Engineering, Nanjing University of Aeronautics and Astronautics, Nanjing, China, in 2016. He is currently pursuing the Ph.D. degree with the School of Automation Science and Electrical Engineering, Beihang University, Beijing, China. His research interests include flight control, missile guidance, and control.

XIAOCEN LIU was born in 1996. She received the B.S. degree from Beihang University, Beijing, China, in 2018. She is currently pursuing the M.S. degree with the School of Automation Science and Electrical Engineering. Her research interests include flight control and multiunmanned aerial vehicle formation.

YUEYANG HUA was born in 1989. He received the Ph.D. degree from Beihang University, in 2019. He is currently an Engineer with the China Academy of Launch Vehicle Technology, Beijing, China. His research interests include sliding-mode control, game theory, robust control, and multiagent system control.

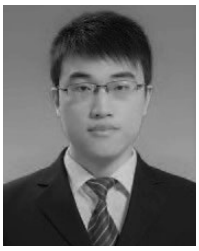

XIAODONG LIU was born in 1987. He received the Ph.D. degree in navigation guidance and control from Beihang University, in 2014. He is currently an Engineer with the Beijing Aerospace Automatic Control Institute, Beijing, China. His research interests include aircraft guidance and control, servo control systems, and so on.

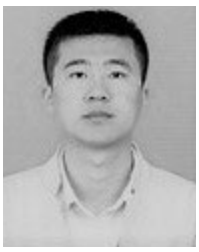

GUOFEI LI was born in 1992. He received the B.S. and M.S. degrees from Lanzhou Jiaotong University, Lanzhou, China, in 2013 and 2016, respectively. He is currently pursuing the Ph.D. degree with the School of Automation Science and Electrical Engineering, Beihang University, Beijing, China. His research interests include nonlinear control, servo system control, cooperative control, and cooperative guidance.